

Rapid evolution of blood-brain-barrier-penetrating AAV capsids by RNA-driven biopanning

Mathieu Nonnenmacher,¹ Wei Wang,¹ Matthew A. Child,¹ Xiao-Qin Ren,¹ Carol Huang,¹ Amy Zhen Ren,¹ Jenna Tocci,¹ Qingmin Chen,¹ Kelsey Bittner,¹ Katherine Tyson,¹ Nilesh Pande,¹ Charlotte Hiu-Yan Chung,¹ Steven M. Paul,¹ and Jay Hou¹

¹Voyager Therapeutics, Cambridge, MA 02139, USA

Therapeutic payload delivery to the central nervous system (CNS) remains a major challenge in gene therapy. Recent studies using function-driven evolution of adeno-associated virus (AAV) vectors have successfully identified engineered capsids with improved blood-brain barrier (BBB) penetration and CNS tropism in mouse. However, these strategies require transgenic animals and thus are limited to rodents. To address this issue, we developed a directed evolution approach based on recovery of capsid library RNA transcribed from CNS-restricted promoters. This RNA-driven screen platform, termed TRACER (Tropism Redirection of AAV by Cell-type-specific Expression of RNA), was tested in the mouse with AAV9 peptide display libraries and showed rapid emergence of dominant sequences. Ten individual variants were characterized and showed up to 400-fold higher brain transduction over AAV9 following systemic administration. Our results demonstrate that the TRACER platform allows rapid selection of AAV capsids with robust BBB penetration and CNS tropism in non-transgenic animals.

INTRODUCTION

Clinical applications of gene therapy in the central nervous system (CNS) are currently limited by the poor transduction of brain and spinal cord by adeno-associated virus (AAV) and other viral vectors.^{1,2} The blood-brain barrier (BBB) represents a formidable obstacle for delivery of AAV into brain tissue following intravenous administration, and even the best-in-class natural BBB-penetrating serotypes, namely AAV9 and other clade F derivatives,^{3,4} only allow limited brain distribution.^{1,5,6} This challenge can be partially overcome by using local delivery routes, such as intraparenchymal injection,^{7,8} intrathecal infusion,⁹ or cisterna magna administration.¹⁰ However, these methods are invasive and only achieve limited distribution and transduction throughout the brain and spinal cord, short of therapeutically desired coverage. These shortcomings could be mitigated by engineered AAV capsids capable of efficiently crossing the BBB via intravascular delivery.

High-throughput mutagenesis and directed evolution of AAV capsids were first described in 2003^{11,12} and are greatly facilitated by the

simplicity of the viral genome organization, extensive knowledge of capsid structure,¹³ and the natural propensity of wild-type AAV to assemble capsids with low mosaicism and high genome-capsid correlation.^{14–16} Early designs of AAV-directed evolution were strictly tailored for *in vitro* selection in cultured cells and used helper adeno-virus coinfection to enrich transduction-competent variants.^{11,12,17,18} Helper-dependent selection is not easily accomplished *in vivo*, and library selection in the mouse initially relied on indiscriminate PCR amplification of AAV genomes from the tissue of interest.¹⁹ Although this approach proved successful to some degree, tremendous effort has been spent on developing new biopanning approaches to efficiently select true positives *in vivo*.^{20,21} Over the past decade, functional AAV library screens based on cell-specific sorting,²² *in vivo* helper virus coinfection,²³ or cell-specific Cre-lox selection^{24–26} have identified improved capsid variants. In particular, two AAV9 variants, PHP.B and PHP.eB, showed an unprecedented ability to transduce C57BL/6 mouse brain via systemic injection.^{26,27} Follow-up studies, however, showed that these properties did not translate to other laboratory mouse strains or to non-human primates (NHPs).^{28–30}

Importantly, Cre-dependent AAV library screening methods^{24–26} strictly rely on transgenic animals for specific recovery of transduction-competent variants, which precludes the use of clinically relevant animals such as NHPs. In this study, we describe TRACER (Tropism Redirection of AAV by Cell-type-specific Expression of RNA), an AAV evolution platform based on recovery of bulk capsid library RNA expressed in a cell-type-specific manner from non-transgenic animal tissue. We used TRACER in a directed evolution screen focused on mouse CNS and were able to isolate multiple capsid

Received 13 September 2020; accepted 16 December 2020;
<https://doi.org/10.1016/j.omtm.2020.12.006>.

Correspondence: Mathieu Nonnenmacher, Voyager Therapeutics, 75 Sidney Street, Cambridge, MA 02139, USA.

E-mail: mnonnenmacher@vygr.com

Correspondence: Jay Hou, Voyager Therapeutics, 75 Sidney Street, Cambridge, MA 02139, USA.

E-mail: jhou@vygr.com

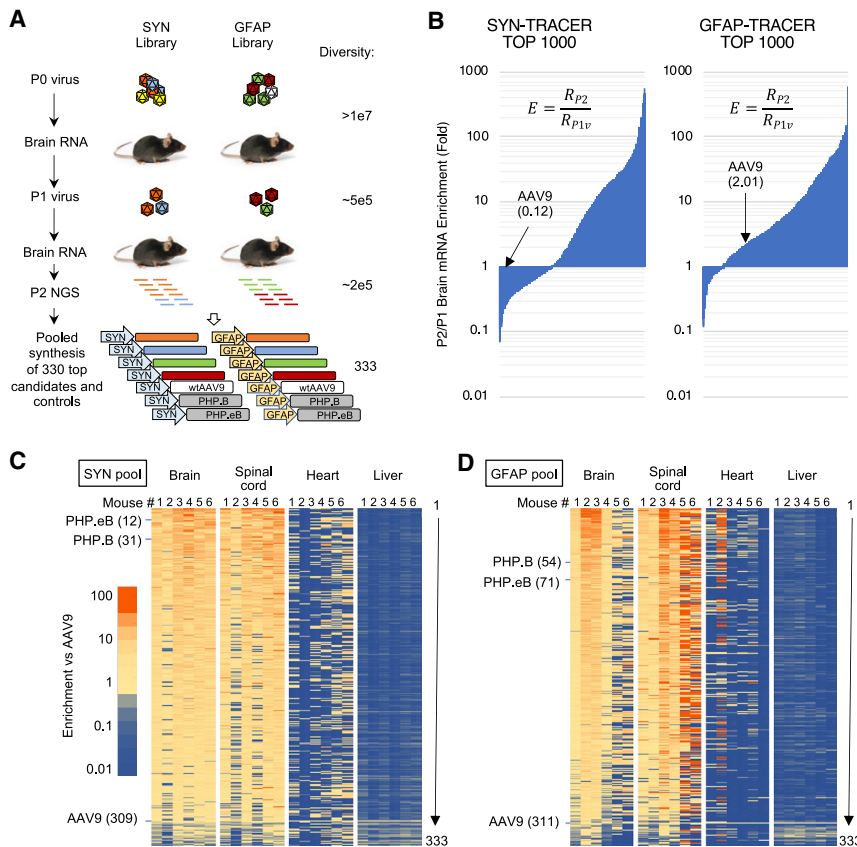


Figure 2. NGS-driven evolution of TRACER libraries in C57BL/6 mice

(A) TRACER workflow and library diversity through successive rounds of evolution and pooled synthesis. Values indicate the number of unique variants detected by NGS. (B) Enrichment analysis of P2 brain RNA. Enrichment score E indicates the relative RNA abundance of each variant (R_{P2}) normalized to P1 virus stock (R_{P1v}). Top 1,000 variants of SYN and GFAP libraries are depicted. (C and D) Fitness analysis of SYN-driven (C) and GFAP-driven (D) pool of 330 capsid candidates plus AAV9, PHP.B, and PHP.eB controls. Heatmaps represent relative RNA enrichment score in brain and spinal cord and DNA enrichment score in heart and liver. Values are normalized to AAV9 control. Numbered columns represent individual animals ($n = 6$). Values represent the average of two codon variants for each mutant and are ranked according to the average of 6 brains. Ranking of control capsids is indicated.

Cap9 Δ plasmid containing a CAP C terminus deletion and in-frame stop codons to eliminate VP1-3 translation (Figure S1).

Capsid libraries were generated by inserting 7-mer randomized peptides between residues 588 and 589 in the hypervariable surface loop VIII³⁵ of AAV9. Random peptides were N-terminally flanked by the original AAV9 residues AQ(587, 588) or by the PHP.eB-derived residues DG(587, 588) or DGT(587, 588, 589) (Figure 1C).²⁷ To avoid the loss of variants resulting from bacterial transformation, library DNA assembled with SYN or GFAP vectors was amplified *in vitro* by rolling circle amplification (RCA) and protomerase end cleavage joining (Figure S1).³⁶ This technique generated large amounts of transfection-ready DNA with a diversity beyond the capacity of our next-generation sequencing (NGS) analysis ($>10^8$ unique variants) and without obvious sequence bias. Viral libraries were produced in HEK293T cells using low-DNA-input conditions to minimize capsid mosaicism and cross-packaging¹⁴ and were administered intravenously to adult C57BL/6 mice ($n = 6$). Whole-brain RNA was isolated after 28 days and capsid library sequences were recovered by RT-PCR. Amplified pools were re-cloned into SYN or GFAP TRACER vectors for a second round of selection (Figure 1D). Abundant capsid amplicons were recovered from all brain samples regardless of the promoter driving the expression (Figure 1E), indicating that

some variants achieve high transduction in the CNS, a tissue with one of the lowest AAV biodistributions.³⁷

Selection of AAV9 capsid variants with enhanced BBB penetration and CNS transduction

NGS analysis was performed after each step of *in vivo* selection to estimate variant diversity and enrichment (Figure 2A). The first round of selection eliminated approximately 95% of variants (from ≥ 10 million to 500,000 unique sequences), and the second round removed 60% of the remaining variants (from 500,000 to 200,000 unique sequences). Enrichment analysis performed after the second round of biopanning showed that hundreds of capsid variants displayed high enrichment scores compared to AAV9 (Figure 2B).

Bioinformatics analysis based on absolute read numbers, enrichment scores, cross-animal consistency, and collapsing of pseudo-variants from sequencing errors led us to select 330 capsid candidates with a favorable CNS enrichment profile (see Materials and methods). Phylogenetic analysis of this brain-enriched variant pool identified several conserved families of variants harboring 9-mer peptides with striking sequence similarities (Figure S2). The largest families clustered in three dominant groups: the most prominent (107 variants) shared the consensus motif DGTxxxGW, a second group (68 variants) displayed the motif DGTxxxP(F/P)(K/R) reminiscent of the PHP.eB capsid and herein referred to as “PHP-like,” and a third group (43 variants) displayed the motif DGTxxxLSS (Figure S2). Smaller groups displayed the motif (DG/AQ)xxxxYD(A/S) or AQxxxxRW (8 and 9 variants, respectively). Of note, we also observed a cluster of 9 variants sharing the motif AQWxxxGY, similar to the recently identified PHP.C2,³⁸ and also one single variant (AQFVVGQY) closely related to the CNS-trophic AAV-F capsid (AQFVVGQSY).²⁵

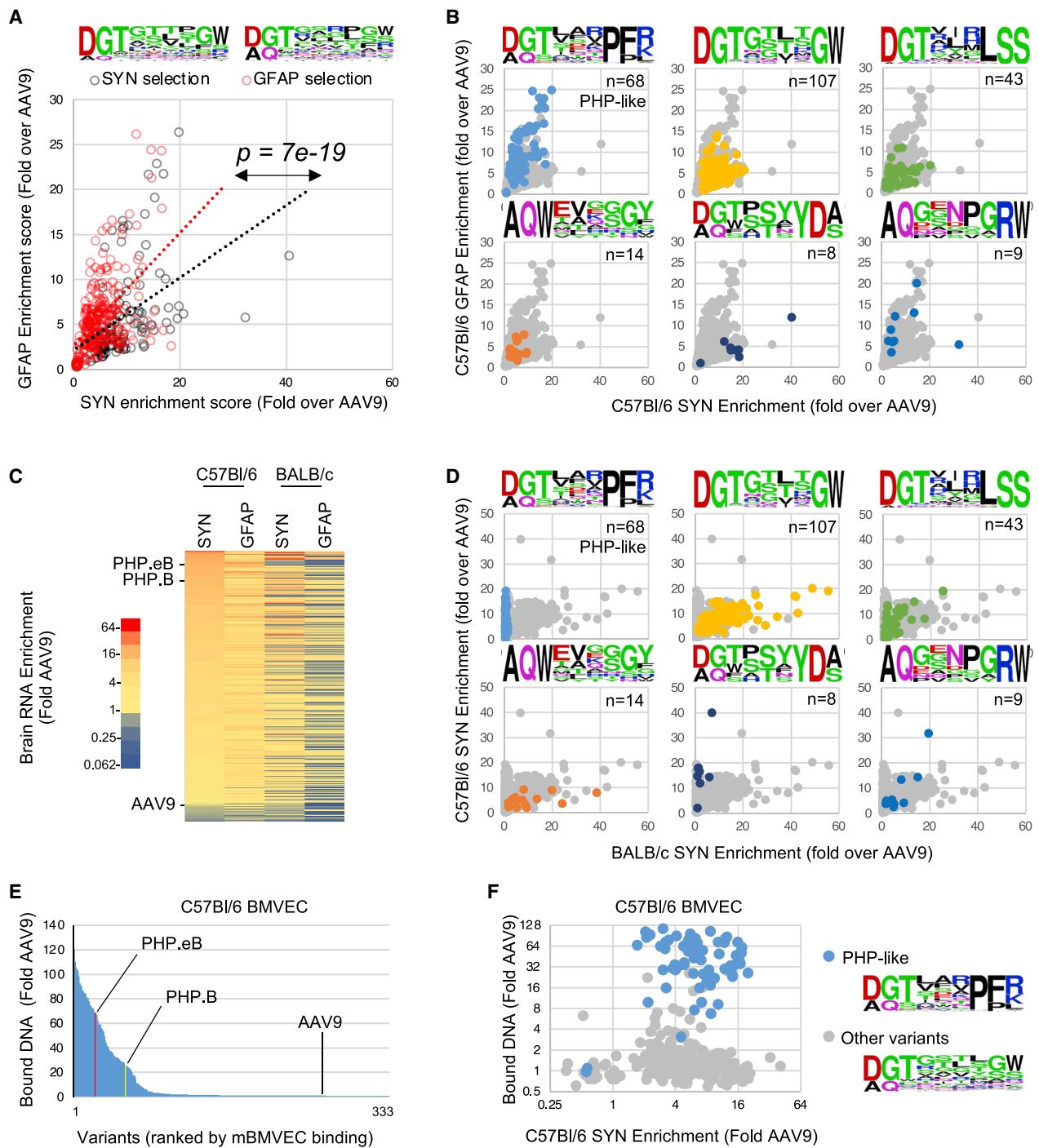


Figure 3. Genotype-to-phenotype analysis of synthetic capsid pool from C57BL/6 CNS biopanning

(A) Comparative neuron and astrocyte fitness of the capsid variants originating from SYN- or GFAP-driven library biopanning (black and red circles, respectively). Each data point represents the average neuron (SYN-driven) and astrocyte (GFAP-driven) RNA enrichment score in i.v.-dosed C57BL/6 mice (n = 6), normalized to AAV9. Linear regression trendline of each population is indicated. p value indicates the statistical difference between the average GFAP-to-SYN score ratio of each subpopulation (unpaired t test). Frequency plots of peptides from SYN- and GFAP-evolved subpools are indicated on top. (B) Enrichment scores of each capsid sequence family in GFAP- (y axis) and SYN-driven RNA assays (x axis). The frequency plots and number of variants in each group are indicated. (C) Comparative brain RNA enrichment of 330 variants in C57BL/6 mice (n = 6) and BALB/c mice (n = 6) following i.v. injection. Color scale indicates the average RNA enrichment score normalized to AAV9. Variants are ranked by SYN-driven RNA enrichment score in C57BL/6 mice. (D) Comparative SYN-driven RNA enrichment score of distinct capsid families in C57BL/6 and BALB/c mice. The

(legend continued on next page)

A synthetic library containing these 330 candidates plus AAV9, PHP.B, and PHP.eB, each encoded as two distinct codon versions (666 nucleotide variants total), was produced *de novo* using pooled primer synthesis as recently described³⁸ and cloned in SYN or GFAP vectors (Figure 2A). Each AAV pool was injected to C57BL/6 mice ($n = 6$), and NGS enrichment analysis was performed 28 days post-injection using RNA from the brain and spinal cord, as well as DNA from heart and liver tissues. Overall, 300 variants showed a brain transduction superior to AAV9, and 92 variants outperformed AAV9 by more than 10-fold (Figures 2C and 2D). By contrast, whereas AAV9 was among the lowest performers in the brain and spinal cord, it showed the highest score in the heart and liver, consistent with CNS cell-type-specific selection conferred by the TRACER platform used in this study (Figures 2C and 2D). The alternative codon versions of each variant showed highly correlated behavior in DNA, virus, and tissue samples, supporting the robustness of the assay (Figure S3). SYN- and GFAP-driven versions of each variant behaved very consistently at the DNA level but diverged at the RNA level (Figure S3), which was not unexpected, since the DNA enrichment is not subject to variations in promoter activity among cell types. Consistent enrichment scores were observed among animals injected with the SYN-driven pool, whereas the GFAP-driven library showed a higher inter-animal variability (Figures 2C and 2D). As expected, both PHP.eB- and PHP.B-positive controls showed a high CNS enrichment score in both screens (Figures 2C and 2D; Data S1). Taken together, the high inter-animal reproducibility, the strong codon variant correlation, and the precise calibration from internal controls allowed us to identify multiple capsids with improved CNS fitness with a very high degree of confidence. Strikingly, despite the absence of effort to select variants with low liver and heart tropism in our screen, the majority of CNS-trophic capsids showed substantial de-targeting from both tissues.

Correlation of variant origin and genotype with *in vivo* and *in vitro* properties

Our synthetic library of 330 brain-enriched variants contained 120 candidates originating from SYN-driven library evolution and 210 candidates from GFAP-driven evolution (Data S1). We asked if the capsid evolution path would favor variants with a bias toward neurons (SYN) or astrocytes (GFAP). When brain RNA enrichment data were stratified according to the library selection method, we observed a significant, albeit modest, transduction bias in favor of the cell type where the library screen was performed (Figure 3A). On average, capsids selected with the GFAP-TRACER library showed a 2-fold increased fitness for astrocyte versus neuron than capsids evolved with the SYN-TRACER library. This relatively modest cell-type specificity likely reflects the absence of negative selection in our screen, combined with the ability of most variants to transduce both neurons and astrocytes, at least to some extent.

We next investigated the impact of capsid sequence on cellular tropism by clustering the neuron/astrocyte fitness of variants with high sequence homology. Although most variants showed improved transduction in both cell types, the PHP-like DGTxxxPF(K/R) group and the AQxxxxRW group showed the highest transduction in astrocytes (Figure 3B). By contrast, variants belonging to the DGTxxxGW sequence group showed no obvious preference for either cell type, and variants belonging to the (DG/AQ)xxxxYD(A/S) group displayed a marked neuronal bias. This observation could suggest that while multiple variants show an increased ability to cross the BBB, the displayed peptide sequence could also modulate the transduction efficiency of different cell types in the brain parenchyma.

We next examined brain transduction in BALB/c mice, since some engineered CNS-trophic capsids have shown substantial variation between C57BL/6 and BALB/c strains due to the usage of a polymorphic receptor on the BBB lumen.^{39–41} Brain RNA enrichment analysis showed that a fraction of variants did not transduce BALB/c brain efficiently, while others showed strong enrichment in both strains (Figure 3C). Strikingly, all PHP-like variants were strictly restricted to C57BL/6 mice and did not outperform AAV9 in BALB/c mice, consistent with previous data obtained with PHP.B and PHP.eB capsids (Figure 3D).^{29,41,42} Similarly, low CNS transduction in BALB/c mice was observed with the capsids from the (DG/AQ)xxxxYD(A/S) group. By contrast, other capsid families showed similar performance across strains (Figure 3D), which strongly suggest the use of different mechanisms to cross the BBB endothelium.

We evaluated the capacity of our 330 variants to bind brain microvascular endothelial cells from C57BL/6 mice (mBMVECs) in culture, a property demonstrated by PHP.B and PHP.eB capsids.⁴¹ Out of the 333 capsids present in the library, 69 showed 10-fold or more binding relative to AAV9 (Figure 3E; Data S1). PHP.B and PHP.eB capsids showed 25- and 68-fold improvement over AAV9, respectively, in agreement with published data.⁴¹ Strikingly, the capsids with high affinity for mBMVECs almost exclusively belonged to the PHP-like cluster (Figure 3F), suggesting that the recapitulation of capsid-receptor interaction in BMVECs is unique to the LY6a-binding variants.^{41,42} Interestingly, capsids from the (DG/AQ)xxxxYD(A/S) group, which share the C57BL/6-specific transduction phenotype with PHP-like capsids, did not bind mBMVECs, suggesting a different receptor usage. Overall, correlation between the *in vivo* performance of capsids and the mBMVEC binding was limited to a unique sequence group (Figure 3F), which clearly indicates that monolayer cultures of BMVECs are a poor predictor of *in vivo* transport across the BBB. Taken together, our data strongly suggest that the TRACER platform identified a broad population of diverse capsid families with distinct BBB transport and brain cell transduction mechanisms, as is evident from their distinct tropism across cell types and mouse strains.

frequency plots and number of variants of each group are indicated. (E) Multiplexed binding assay of synthetic capsid pool to C57BL/6 mouse primary brain microvascular endothelial cells (BMVECs). Values indicate bound viral DNA enrichment score relative to AAV9. Ranking of reference PHP.eB, PHP.B, and AAV9 capsids is indicated. (F) Scatterplot presenting the correlation between virus binding to mouse BMVECs and C57BL/6 brain RNA enrichment scores. The PHP-like capsid variants are indicated by blue dots, all other variants by gray dots.

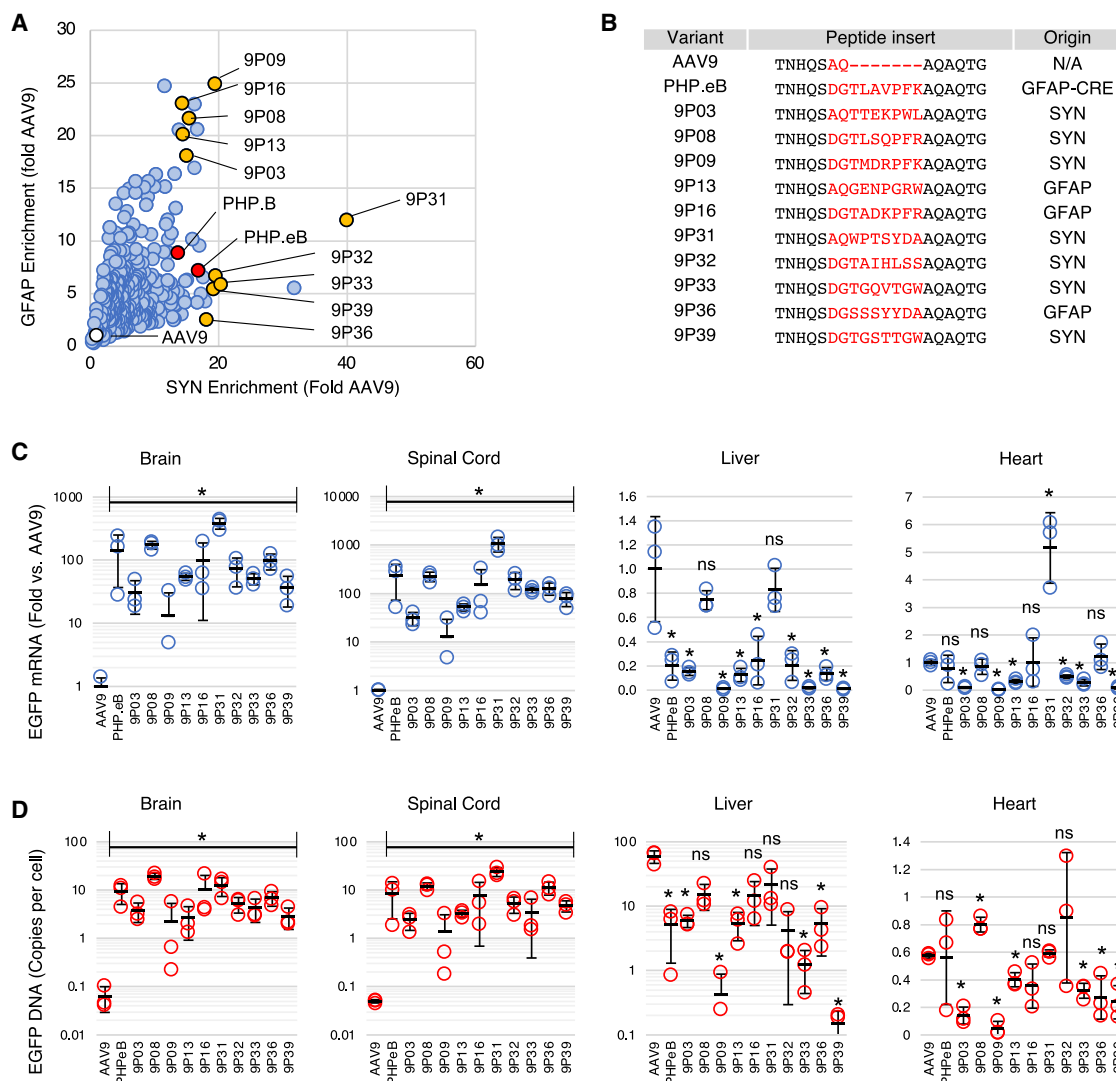


Figure 4. Individual characterization of TRACER capsid candidates

(A) Brain RNA enrichment score of pooled synthetic variants in the SYN- and GFAP-driven assay. Values are normalized to AAV9. Yellow dots indicate candidates chosen for individual testing; red and white dots indicate the PHP and AAV9 control capsids, respectively. (B) Sequence of capsids selected for individual characterization. The right column indicates the biopanning method used to evolve each variant. (C) Real-time RT-PCR analysis of EGFP transgene RNA expression in the brain, spinal cord, liver, and heart 28 days after i.v. injection of each capsid in C57BL/6 mice (4×10^{11} VG per mouse, $n = 3$). Values indicate mean \pm SD ($n = 3$), normalized to AAV9. * $p < 0.05$ relative to AAV9 (unpaired t test); ns, not significant. (D) AAV genome biodistribution measured by qPCR. Values indicate mean \pm SD ($n = 3$) EGFP copies per diploid cell. * $p < 0.05$ relative to AAV9 (unpaired t test); ns, not significant. All brain and spinal cord samples were statistically different from AAV9.

In vivo characterization of selected AAV capsid candidates

Ten capsid candidates were selected for individual evaluation, based on high CNS enrichment scores in either the SYN or GFAP screen (Figure 4A) and sequence divergence (Figure 4B). Each capsid was used to produce recombinant AAV containing a self-complementary⁴³ EGFP reporter driven by the ubiquitous CAG promoter and administered intravenously to C57BL/6 mice at a dose of 4×10^{11} viral genomes (VG) per animal. AAV9 and PHP.eB were used as references. Relative EGFP mRNA expression was measured 4 weeks post-injection. All 10 candidates largely outperformed AAV9 in the brain and spinal cord

(Figure 4C). When compared to AAV9, EGFP expression in the CNS was increased from 13-fold (9P09) to 385-fold (9P31). In the spinal cord, 9P31 transduction was more than 1,000-fold higher than AAV9. By comparison, PHP.eB transduction was 144-fold higher than AAV9 in the brain and 236-fold higher in the spinal cord, in agreement with the published data.²⁷ Of note, the qPCR scores from individual capsids showed a high correlation with the SYN screen, but not with the GFAP screen, indicating that SYN-driven expression was more predictive of global brain transduction (Figure S4). As suggested by our NGS analysis, no capsid variant transduced the liver better than

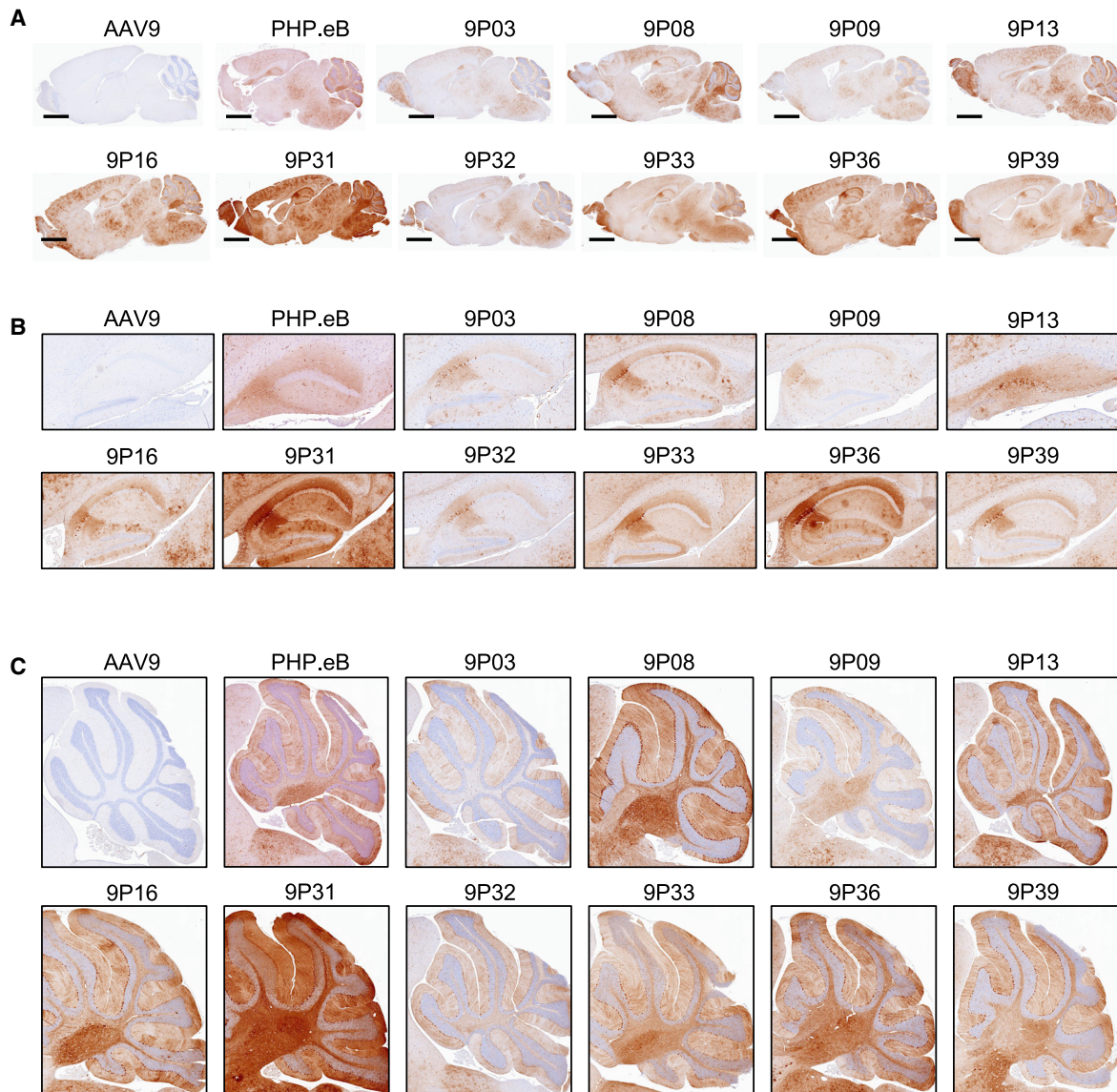


Figure 5. Brain transduction profile of TRACER capsid candidates in adult mice

EGFP was detected by immunohistochemistry (IHC) from formalin-fixed paraffin-embedded (FFPE) sections in the brain of adult C57BL/6 mice 28 days after i.v. infusion with 4×10^{11} VG per mouse. (A–C) Representative images of whole-brain sagittal sections (A), hippocampus (B), and cerebellum (C) are shown. Scale bar in (A), 2 mm.

AAV9; instead, some variants (9P09, 9P33, and 9P39) were de-targeted by approximately 100-fold. In the heart, no capsid variants outperformed AAV9 with the exception of 9P31, which showed a 5-fold increase in RNA expression (Figure 4C, right panel).

Biodistribution of AAV genomes showed a pattern similar to RNA expression (Figure 4D). The CNS biodistribution of novel variants ranged from 2 VG per cell (9P03 and 9P09) to 20–25 VG per cell (9P08 and 9P31). Biodistribution of PHP.eB (8.6 and 9.3 VG per cell in the brain and spinal cord, respectively) was in the expected range.^{26,27} By comparison, mice injected with AAV9 showed less than 0.1 VG per cell in the brain and spinal cord (Figure 4D). Consistent with the RNA

data, 9P09 and 9P39 showed a very low DNA biodistribution in the liver (<1 VG per cell) relative to AAV9 (~ 60 VG per cell).

We then analyzed EGFP protein expression in brain sagittal sections by immunohistochemistry. All the TRACER-evolved capsids showed strong and widespread EGFP expression throughout the entire brain (Figure 5A). As expected from the RNA quantitation data, capsids 9P03 and 9P09 showed the lowest transduction; capsids 9P08, 9P16, 9P33, and 9P36 were similar to PHP.eB; and capsid 9P31 showed a strikingly high EGFP expression in all brain regions (Figure 5A). Similar results were obtained by observing native EGFP fluorescence in frozen sections from the same animals

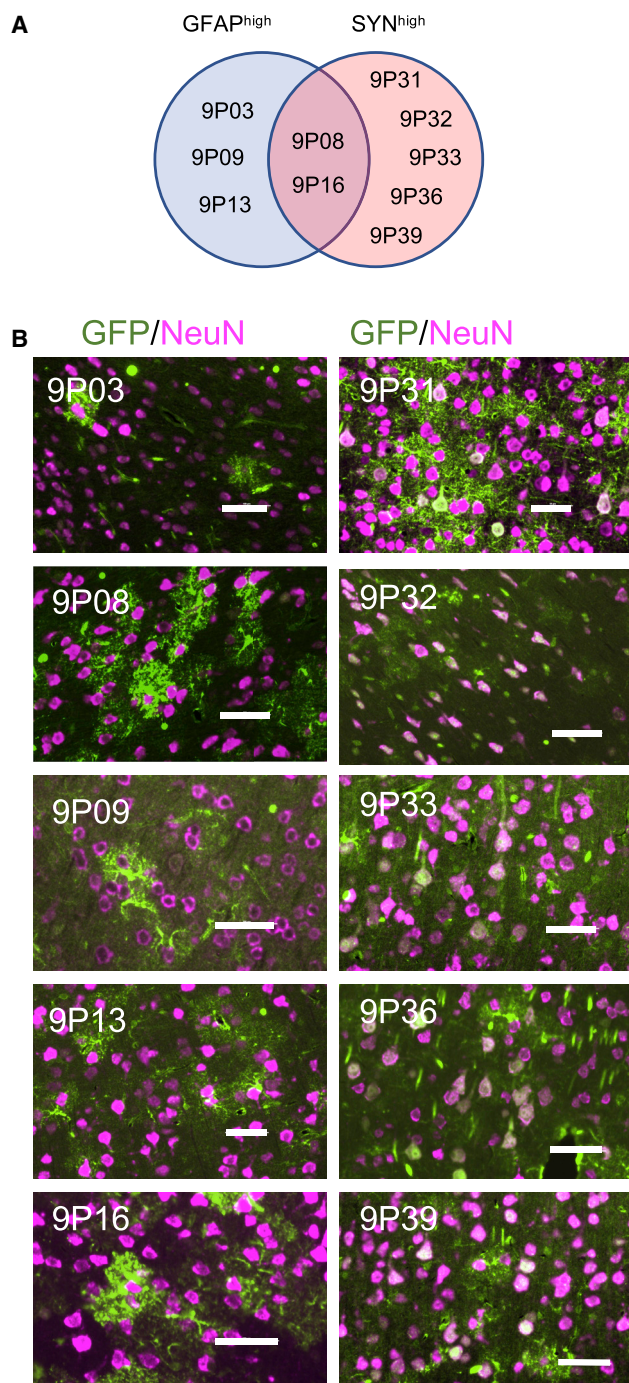


Figure 6. Cortical neuron transduction by TRACER capsid candidates in adult mice

(A) Relative fitness of TRACER capsids in the GFAP-driven and SYN-driven library NGS assay. (B) EGFP (green) and NeuN (magenta) were detected by IHC from FFPE sections in the brain of adult C57BL/6 mice 28 days after intravascular infusion with 4×10^{11} VG per mouse. Representative images of cortex are shown. Bar, 50 μm .

(Figure S5). Despite different transgene expression levels, all capsid variants showed a similar spatial distribution characterized by preferential transduction of the cerebellum, brain stem, medulla, pons, hippocampus, thalamus, cortex, anterior olfactory nucleus, and olfactory bulb (Figure 5A; Figure S6). Notably, all capsid variants showed a strong transduction of the CA2 region of the hippocampus (Figure 5B) and of the Purkinje and molecular layers of the cerebellum (Figure 5C).

All engineered capsids demonstrated a predominant tropism for neuronal cells in the hippocampus, as demonstrated by NeuN immunostaining (Figure S7). By contrast, differences in cellular tropism were observed in the cortex and the thalamus regions, where some variants showed an obvious neuronal preference (9P31, 9P32, 9P33, 9P36, and 9P39), whereas others (9P03, 9P08, 9P09, 9P13, and 9P16) transduced mostly NeuN-negative cells with distinctive highly branched morphological features (Figure 6; Figure S7). Capsids with marked neuronal preference were also the strongest performers in the SYN-driven NGS RNA enrichment assay (Figure 6A). Intriguingly, capsids with high performance in the GFAP-driven RNA assay did not appear to efficiently transduce GFAP-positive astrocytes in the cortex, thalamus, or hippocampus, possibly suggesting a preferred tropism for immature or protoplasmic astrocytes rather than mature GFAP⁺ astrocytes. Similarly, despite a strong transduction of the entire cerebellum, all variants appeared to be restricted to Purkinje cells and did not transduce the GFAP⁺ Bergmann glia (Figure S8).

DISCUSSION

Here, we developed a transcription-dependent platform that allowed rapid selection of AAV capsid variants with high CNS tropism. Our platform does not require the use of transgenic animals and is, therefore, compatible with virtually all *in vivo* models, including higher mammals.

Directed evolution strategies relying on total viral DNA recovery can suffer from the confounding effects of virus productivity bias or the carryover of inert particles accumulated in the tissue of interest.^{20,21} In our case, using RNA expression as an obligatory step allowed a reliable selection of true positives, attested by the improvement of all our individually tested candidates by at least one order of magnitude over AAV9. In addition, the use of cell-type-specific promoters presumably reduced the recovery of capsids from undesired cell types and contributed to the rapid emergence of variants with high neuronal or glial tropism after only two rounds of screening. It is noteworthy that our screen did not uncover capsids with a strict tropism for brain endothelial cells, which constituted the dominant species in a previous DNA-based brain library screen.⁴⁴ The TRACER system can be adapted to any promoter sequence of less than 2 kb, to accommodate the size limit allowed by AAV packaging, and may be of great value in numerous applications where selective recovery from rare cell types is required.

Another key aspect of our study was the identification of classes of conserved variants with similar properties, in agreement with a recent report.³⁸ This is important when considering the undersampling of

AAV libraries. Consistent with previous observations,¹⁴ our AAV libraries contained about 2e7 unique variants regardless of the initial DNA library diversity. For a 7-mer random library (1.28e9 theoretical variants), the probability for any given variant to be present in the original pool is therefore less than 2%. However, if one or more amino acid substitutions is tolerated, the likelihood for recovering a biochemically similar capsid increases dramatically. We identified, among many others, more than 60 variants harboring a peptide motif similar to PHP.B and PHP.eB capsids, as well as close homologs to the recently identified AAV-F and PHP.C2 capsids.^{25,38} The fact that our screen “re-discovered” close homologs of multiple capsids previously identified using several independent Cre-Lox selections, in addition to novel variants with unprecedented CNS transduction, suggests that the sequence space coverage and the robustness of the TRACER platform are equivalent or possibly superior to the existing transgenic evolution platforms.

The SYN-driven NGS analysis data were highly predictive of individual capsid properties and identified multiple variants with a high tropism for neurons. By comparison, capsids with high enrichment score in the GFAP-driven assay showed lower inter-animal and inter-assay consistency and did not transduce GFAP-positive astrocytes efficiently. These observations could suggest a disconnect between the cellular tropism of certain capsid variants and the specificity of the synthetic gfaABC1D promoter used to drive library mRNA expression. If capsids predominantly transduce non-astrocytic cells, nonspecific transcription from the gfaABC1D promoter⁴⁵ could result in positive but inconsistent RNA recovery. In addition, the recently described neuronal preference of the CBA promoter⁴⁶ (similar to the CAG used in our individual capsid study) could lead to an underestimation of capsid tropism for non-neuronal cells. Regardless, the high success ratio of individual capsid candidates (10/10 candidates with at least 10-fold improvement over AAV9) argues for the robustness of our cell-type-specific NGS platform.

Variants from different sequence clusters showed qualitative and quantitative variation in their cellular tropism and mouse strain restriction, which strongly suggest the use of multiple mechanisms for transport across the BBB. Brain tissue examination, however, showed that all candidates had a strikingly similar tropism for specific brain regions such as the hippocampus CA2 region, the cerebellum, or the thalamus. This repeated pattern, also shared by PHP.B and AAV-F capsids,^{25,26} suggest that while the 7-mer peptide insertion is critical for transport across the BBB, other AAV9 capsid domains also contribute to the regional distribution of the virus regardless of the BBB translocation mechanism. This finding underlies the multifactorial nature of *in vivo* transduction and could have important implications for future library designs.

MATERIALS AND METHODS

TRACER vectors construction

Library shuttle vectors harboring an AAV capsid expression cassette under the control of the human Synapsin 1 promoter³³ or the gfaABC1D promoter³⁴ were assembled using standard molecular

biology techniques, and full sequences are available in the [Supplemental information](#). These plasmids contain full-length inverted terminal repeats (ITRs) as well as minimal AAV *cis* sequences required for capsid mRNA expression and splicing during virus production. The capsid fragment extending from the hypervariable loop VIII to the stop codon was removed and replaced by a unique BsrGI restriction site used for library insertion. TelN protelomerase palindromic recognition sites (TATCAGCACACAATTGCCATTATACGCGCGTATAATGGAC TATTGTGTGCTGATA) were inserted outside of the ITRs to allow concatemer resolution and end joining after cloning-free library amplification (see below). The helper vector pREP-3stop encoding the REP protein *in trans* was generated by MscI digestion and self-ligation of a pREP2-CAP9 plasmid, in order to delete nucleotides 1514–2030 of AAV9 VP1. Artificial stop codons were added downstream of the start codons of VP1, VP2, and VP3. The amino acid sequence of the assembly-activating protein (AAP) was kept unchanged. The full sequence of this construct is available in the [Supplemental information](#).

AAV library construction and virus production

Primers 9L8-F24, 9DGL8-F24, and 9GDTL8-F24 containing hand-mixed randomized NNK codons flanked by conserved sequences ([Table S1](#)) were generated by Integrated DNA Technologies (IDT, Coralville, IA, USA) and used together with the CAP9-StopR23 primer to generate library amplicons containing a randomized loop embedded in a fragment covering nucleotides 1735–2211 of AAV9 VP1. A gBlock fragment (IDT) was used as a template to prevent carryover from plasmid material in subsequent reactions. PCR was performed for 15 cycles using Q5 polymerase (New England Biolabs [NEB], Ipswich, MA, USA). The resulting amplicons were gel purified, and 500 ng of each amplicon was assembled with 2 µg of BsrGI-digested TRACER vectors using 100 µL 2× NEBuilder mix (NEB). Assembled products were treated with T5 exonuclease to eliminate unassembled DNA and purified on DNA Clean and Concentrator-5 columns (Zymo Research, Irvine, CA, USA). The resulting products were quantified by nanodrop, and the entire reaction (routinely 500–600 ng) was used in a 900 µL rolling circle amplification reaction performed at 30°C overnight with TruePrime RCA kit (4Basebio, Madrid, Spain). The reaction was heat-inactivated 10 min at 65°C, diluted 1:5 in 1× ThermoPol buffer (NEB), and treated at 30°C for 1 h with 50 µL of protelomerase (NEB) to obtain linear closed-end DNA monomers. After heat inactivation of protelomerase at 70°C for 10 min, a 5 µL aliquot (~1:1,000 of the total reaction) was run on an agarose gel to confirm amplification and complete concatemer resolution. Qiaprep 2.0 columns (QIAGEN) were used for final DNA purification. The procedure routinely yielded ~200 µg of transfection-ready dogbone DNA.

Virus production was performed in HEK293T maintained in Dulbecco's modified Eagle's medium with GlutaMAX, penicillin/streptomycin (all from Gibco) and 5% fetal bovine serum (Corning). Calcium phosphate transfection was performed using 15 µg pAdDeltaF6 adenovirus helper plasmid, 10 µg pREP-3stop, and 1 µg library DNA per dish. These conditions have been previously shown to allow optimal virus yields, library diversity, and DNA-capsid correlation.¹⁴

Cells and culture medium were harvested 72 h after transfection by scraping. Cells were pelleted by low-speed centrifugation and lysed by addition of 0.1% Triton X-100 (Thermo Scientific), while supernatant was precipitated on ice with 1:10th volume of a 40% PEG-8000, 2.5 M NaCl solution followed by centrifugation. Lysate and supernatant fractions were pooled and fractionated on two successive rounds of iodixanol gradients as previously described.⁴⁷ Buffer exchange was performed on Amicon-100 columns (Millipore) with phosphate-buffered saline containing 200 mM total NaCl and 0.001% Pluronic F-68 (Gibco), and the final virus samples were analyzed by real-time PCR using a REP-specific primer/probe set (Table S1). Final virus preparations were tested by silver stain of PAGE gels and Endo-safe endotoxin assay (Charles River Laboratories, Wilmington, MA, USA).

Animals

Adult male C56Bl/6J mice (22–30 g; 7–8 weeks; stock #027) were purchased from the Charles River Laboratory. Adult male BALB/C mice (22–30 g; 7–8 weeks; #000651) were purchased from The Jackson Laboratory (Bar Harbor, ME, USA). Animals were housed in a 12-h light:12-h dark environment and provided food and water *ad libitum*. All animal protocols were approved by the Voyager Therapeutics (Cambridge, MA, USA) Institutional Animal Care and Use Committee (IACUC). For all experiments, animals were maintained in the animal colony for 1 week before dosing, and all animals were euthanized using a ketamine/xylazine cocktail.

Library screening by *in vivo* selection

AAV libraries were injected to C57BL/6 mice ($n = 3$) at a dose of 1e12 VG per animal into the lateral tail vein. For multiplexed analysis of synthetic libraries, 5e11 VG were injected to each C57BL/6 ($n = 6$) and BALB/c mouse ($n = 6$). Animals were euthanized 28 days post-injection and perfused with cold PBS. Brain, spinal cord, heart, and liver were promptly collected, snap-frozen in liquid nitrogen, and stored at -80°C .

Whole-brain RNA was extracted using the RNeasy plus universal kit (QIAGEN) following manufacturer's instructions, and mRNA was purified using Oligotex beads (QIAGEN). Reverse transcription was performed with the gene-specific CAP-RT primer (Table S1) using Superscript IV first-strand synthesis kit (Life Technologies). Full-length spliced capsid cDNA was then amplified for 25 cycles using SpliceF6 and CAP-RT primers in multiple 50 μL PCR reactions containing 4 μL of cDNA and 25 μL Q5 HotStart high-fidelity 2 \times master mix (NEB). Gel-purified amplicons were used in nested PCR reactions for cloning into TRACER SYN or GFAP vectors (using CAP9-L8F and CAP9-StopR23 primers) or for generation of NGS templates (using 9*NGS-F and 9*NGS-R primers).

In vivo characterization of TRACER AAV variants

REP-CAP plasmids containing various capsid candidates were generated from an ITR-less REP2-CAP9-BsrGI plasmid, and virus production was performed by co-transfection of HEK293T with 15 μg pAd-DeltaF6 adenovirus helper plasmid, 10 μg REP-CAP plasmid, and

5 μg self-complementary AAV CAG-EGFP plasmid (Supplemental information). Cell harvesting and lysis, iodixanol gradient purification, and buffer exchange were performed as described for libraries. Final virus titers were determined by TaqMan real-time PCR using a EGFP primer/probe set (Life Technologies).

Twelve capsid variants including AAV9 and PHP.eB were injected, respectively, into the lateral tail vein (4e11 vg per animal). Three mice were used for mRNA extraction and three mice for immunohistochemistry staining. Animals were euthanized 28 days post-injection. Animals assigned for mRNA extraction were perfused with cold PBS, and tissues were snap-frozen in liquid nitrogen. Animals assigned for immunohistochemistry were perfused with cold PBS and 4% paraformaldehyde (PFA), and tissues were immersion-fixed in 10% neutral formalin and cryo-preserved in sucrose. Brains were sectioned in half following the sagittal midline. One hemisphere was frozen in OCT and sectioned with a cryostat for EGFP direct observation and whole-slide scanning, and the other hemisphere was processed for paraffin embedding.

Immunohistochemistry and imaging

Frozen right brain hemispheres were sectioned at 10 μm thickness on a cryostat (Leica Biosystems) and mounted on glass slides with Prolong Gold anti-fade mountant (Thermo Fisher Scientific, cat. P36934). Left hemispheres were fixed in 4% paraformaldehyde at room temperature for 24 h and processed for paraffin embedding and 5 μm thickness sectioning. Antigen retrieval was performed at 95°C for 40 min with CC1 (Ventana). Rabbit anti-GFP (A-11122, Invitrogen) was incubated for 60 min at 1:250 dilution in antibody diluent (PBS with 10% normal goat serum and 0.01% Triton X-100), followed by 16 min incubation with OmniMap anti-Rabbit HRP (Ventana #760-4311). Signal was detected with 3,3'-diaminobenzidine ChromoMap DAB kit (Ventana), and counterstaining was performed with hematoxylin II and bluing reagent (Ventana) before slides were dehydrated and mounted in Cytoseal 60 (Thermo Scientific). Immunofluorescence for NeuN-EGFP or EGFP-GFAP was performed on a Ventana Discovery Ultra autostainer. All the incubations were at 37°C unless otherwise stated. Antigen retrieval was performed at 95°C for 40 min with Ventana CC1. Rabbit anti-NeuN (ABN78, Millipore), rabbit anti-GFAP (Z0334, Dako) and rabbit anti-GFP (see above) were used at 1:3,000, 1:400, and 1:250 dilution, respectively. This was followed by 16 min incubation with OmniMap anti-rabbit horseradish peroxidase (HRP) and signal detection with Cy5, rhodamine, or fluorescein isothiocyanate (FITC) discovery reagents (Ventana). Slides mounted in Cytoseal 60 were imaged on a Nikon Eclipse Ti-2 epifluorescence microscope.

NGS and bioinformatics analysis

NGS amplicon libraries were generated by 15 cycles of nested PCR with Q5 High-Fidelity DNA Polymerase (NEB) using 9*NGS-F and 9*NGS-R primers. PCR products were separated on 3.0% agarose gel and purified with Zymo Gel DNA Recovery Kit (Zymo Research). Final NGS libraries were quantified with Qubit dsDNA HS kit (Life Technology). Samples were spiked with 20% PhiX libraries

(Illumina), denatured with 0.2 N NaOH at room temperature for 5 min, further diluted with HT1 buffer, and subjected to Illumina Nextseq500 analysis with 75-cycle or 150-cycle high-output kit.

A custom AAV amplicon-sequencing pipeline was developed to process the NGS raw data from round 1 and round 2 screens. Briefly, raw reads were first quality filtered, and a sequential trimming (<https://sourceforge.net/projects/bbmap/>) was applied to map invariable flanking sequences allowing a 10% error rate. Variable library inserts were length filtered (27 nt) for peptide translation. Inserts with nucleotide sequences within 1 Levenshtein distance to the relatively abundant ones were collapsed to reduce sequencing and PCR errors.⁴⁸ T/G filtering of every third position of NNK codons was also applied to filter out sequencing errors.

For round 2 enrichment analysis, the reads per million (rpm) of each capsid variant in brain RNA recovery was divided by the rpm of this variant in P1 virus pool. The list of 330 candidates were selected based on: (1) raw count of the variant in virus input (>10), and (2) fold change between P2 brain RNA recovery and P1 virus stock (>20). In total, 330 unique capsid variants were kept for primer pool synthesis and round 3 characterization studies. A mammalian NNK and NNM codon table was applied to generate non-rare codon variants of each peptide. To process the data from round 3 synthetic library analysis, NNK and NNM codon sequences of 330 capsid variants plus PHP.eB and PHP.B were built by bowtie index as reference genome.⁴⁹ The minimal hamming distance⁵⁰ of the 664 codon sequences was 2. Sequence reads of inserts were aligned to bowtie references with 1 mismatch allowed.

Vector mRNA and DNA quantification in mouse tissue

For transgene mRNA quantification, total RNA was extracted from 100–200 mg of tissue using RNeasy plus universal kit (QIAGEN), and reverse transcription was performed with 1 µg RNA using the Quantitect kit (QIAGEN). Spliced EGFP transcripts were quantified by TaqMan PCR using a primer-probe set specific for CMV-globin exon-exon junction (Table S1). Murine TATA box-binding protein (TBP) RNA was used as a housekeeping control in all experiments. Relative expression levels were calculated from the ΔC_t values and normalized to AAV9 samples.

For vector DNA quantification, 20 mg tissue was processed using the Blood and Tissue DNeasy kit (QIAGEN). Concentration was adjusted to 40 ng/µL in all samples, and 100 ng was used for TaqMan PCR quantification with a probe/primer set specific for EGFP (Life Technologies). Normalization was performed with a TaqMan set specific for the murine TERT gene (Life Technologies; Table S1).

In vitro binding and transduction assays

Recombinant AAV9 containing CAG-, SYN-, or GFAP-driven EGFP, as well as AAV9 TRACER vectors containing CAG-, SYN-, or GFAP-driven CAP, were generated as described above. Primary mixed neuronal culture was prepared with brains from embryonic day 17 CD1 mice (Charles River Laboratories). Dissociated hippocampal

neurons were plated onto poly-D-lysine coated plates at 100,000 cells/well and cultured in neurobasal media supplemented with B27, GlutaMAX, and penicillin/streptomycin (Gibco). Cells were transduced at day *in vitro* 4. HEK293T cells and primary mixed neuronal cells were transduced 48 h with 1e5 VG per cell. Total RNA was extracted using RNeasy mini columns (QIAGEN), and reverse transcription was performed with a Quantitect kit (QIAGEN). Expression levels of EGFP transcripts or CAP transcripts were measured with the same TaqMan primer/probe set specific for the CMV-globin exon-exon junction (Table S1). Murine TBP and human Glyceraldehyde 3-phosphate dehydrogenase (GAPDH) were used as housekeeping controls in mouse primary brain cells and HEK293T cells, respectively. Primary murine C57BL/6-derived BMVECs were obtained from Cell Biologics (Chicago, IL, USA) and cultured with endothelial media from the same source. Synthetic AAV library was added in culture medium for 2 h at 37°C before extensive PBS washes. Cells were then lysed directly in the flask, and low-molecular-weight DNA was extracted using Zyppy miniprep columns (Zymo Research). Viral DNA was amplified for 20 cycles with primers containing Illumina adapters and gel purified for NGS sequencing.

Statistical analysis

Unpaired two-tailed t tests were performed in Excel and are reported in figure legends. A p value < 0.05 was considered significant. Results are reported as mean ± SD. Correlation and R² values were calculated in Excel.

SUPPLEMENTAL INFORMATION

Supplemental Information can be found online at <https://doi.org/10.1016/j.omtm.2020.12.006>.

ACKNOWLEDGMENTS

This study was funded by Voyager Therapeutics.

AUTHOR CONTRIBUTIONS

M.N. designed and performed experiments, analyzed data, prepared figures, and wrote the manuscript. W.W. developed pipelines and performed bioinformatics analysis of NGS data, helped with data analysis, and assisted with manuscript preparation. M.A.C. and A.Z.R. performed experiments, virus production, and characterization. X.-Q.R. performed NGS runs. C.H., Q.C., and J.T. performed *in vivo* dosing and tissue processing. N.P., K.B., and K.T. performed tissue processing and IHC imaging. C.H.-Y.C. performed experiments with mouse primary cells. S.M.P. provided support and oversight. J.H. helped with study design, data analysis, and manuscript preparation and supervised the project. All authors approved the manuscript.

DECLARATION OF INTERESTS

M.N., W.W., M.A.C., X.-Q.R., C.H., A.Z.R., J.T., K.B., K.T., N.P., C.H.-Y.C., and J.H. are paid employees of Voyager Therapeutics Inc. Voyager has filed a patent application related to the subject matter of this paper: WO2020072683. S.M.P. currently serves on the

board of Voyager Therapeutics, Sage Therapeutics, Karuna Therapeutics, and Alnylam Pharmaceuticals.

REFERENCES

- Deverman, B.E., Ravina, B.M., Bankiewicz, K.S., Paul, S.M., and Sah, D.W.Y. (2018). Gene therapy for neurological disorders: progress and prospects. *Nat. Rev. Drug Discov.* *17*, 641–659.
- Gray, S.J., Woodard, K.T., and Samulski, R.J. (2010). Viral vectors and delivery strategies for CNS gene therapy. *Ther. Deliv.* *1*, 517–534.
- Mendell, J.R., Al-Zaidy, S., Shell, R., Arnold, W.D., Rodino-Klapac, L.R., Prior, T.W., Lowes, L., Alfano, L., Berry, K., Church, K., et al. (2017). Single-dose gene-replacement therapy for spinal muscular atrophy. *N. Engl. J. Med.* *377*, 1713–1722.
- Ellsworth, J.L., Gingras, J., Smith, L.J., Rubin, H., Seabrook, T.A., Patel, K., Zapata, N., Olivieri, K., O'Callaghan, M., Chlipala, E., et al. (2019). Clade F AAVHSCs cross the blood brain barrier and transduce the central nervous system in addition to peripheral tissues following intravenous administration in nonhuman primates. *PLoS One* *14*, e0225582.
- Wang, D., Tai, P.W.L., and Gao, G. (2019). Adeno-associated virus vector as a platform for gene therapy delivery. *Nat. Rev. Drug Discov.* *18*, 358–378.
- Hocquemiller, M., Giersch, L., Audrain, M., Parker, S., and Cartier, N. (2016). Adeno-Associated Virus-Based Gene Therapy for CNS Diseases. *Hum. Gene Ther.* *27*, 478–496.
- Taymans, J.-M., Vandenberghe, L.H., Van den Haute, C., Thiry, I., Deroose, C., Mortelmans, L., et al. (2007). Comparative analysis of adeno-associated viral vector serotypes 1, 2, 5, 7, and 8 in mouse brain. *Hum. Gene Ther.* *18*, 195–206, <https://doi.org/10.1089/hum.2006.178>.
- Cearley, C.N., and Wolfe, J.H. (2006). Transduction characteristics of adeno-associated virus vectors expressing cap serotypes 7, 8, 9, and Rh10 in the mouse brain. *Mol. Ther.* *13*, 528–537.
- Hinderer, C., Bell, P., Katz, N., Vite, C.H., Louboutin, J.P., Bote, E., Yu, H., Zhu, Y., Casal, M.L., Bagel, J., et al. (2018). Evaluation of Intrathecal Routes of Administration for Adeno-Associated Viral Vectors in Large Animals. *Hum. Gene Ther.* *29*, 15–24.
- Hinderer, C., Bell, P., Vite, C.H., Louboutin, J.P., Grant, R., Bote, E., Yu, H., Pukenas, B., Hurst, R., and Wilson, J.M. (2014). Widespread gene transfer in the central nervous system of cynomolgus macaques following delivery of AAV9 into the cisterna magna. *Mol. Ther. Methods Clin. Dev.* *1*, 14051.
- Perabo, L., Büning, H., Kofler, D.M., Ried, M.U., Girod, A., Wendtner, C.M., Enssle, J., and Hallek, M. (2003). In vitro selection of viral vectors with modified tropism: the adeno-associated virus display. *Mol. Ther.* *8*, 151–157.
- Müller, O.J., Kaul, F., Weitzman, M.D., Pasqualini, R., Arap, W., Kleinschmidt, J.A., and Trepel, M. (2003). Random peptide libraries displayed on adeno-associated virus to select for targeted gene therapy vectors. *Nat. Biotechnol.* *21*, 1040–1046.
- Xie, Q., Bu, W., Bhatia, S., Hare, J., Somasundaram, T., Azzi, A., and Chapman, M.S. (2002). The atomic structure of adeno-associated virus (AAV-2), a vector for human gene therapy. *Proc. Natl. Acad. Sci. USA* *99*, 10405–10410.
- Nonnenmacher, M., van Bakel, H., Hajjar, R.J., and Weber, T. (2015). High capsid-genome correlation facilitates creation of AAV libraries for directed evolution. *Mol. Ther.* *23*, 675–682.
- Schmit, P.F., Pacouret, S., Zinn, E., Telford, E., Nicolaou, F., Broucque, F., Andres-Mateos, E., Xiao, R., Penaud-Budloo, M., Bouzelha, M., et al. (2019). Cross-Packaging and Capsid Mosaic Formation in Multiplexed AAV Libraries. *Mol. Ther. Methods Clin. Dev.* *17*, 107–121.
- Körbelin, J., Hunger, A., Alawi, M., Sieber, T., Binder, M., and Trepel, M. (2017). Optimization of design and production strategies for novel adeno-associated viral display peptide libraries. *Gene Ther.* *24*, 470–481.
- Grimm, D., Lee, J.S., Wang, L., Desai, T., Akache, B., Storm, T.A., and Kay, M.A. (2008). In vitro and in vivo gene therapy vector evolution via multispecies interbreeding and retargeting of adeno-associated viruses. *J. Virol.* *82*, 5887–5911.
- Maheshri, N., Koerber, J.T., Kaspar, B.K., and Schaffer, D.V. (2006). Directed evolution of adeno-associated virus yields enhanced gene delivery vectors. *Nat. Biotechnol.* *24*, 198–204.
- Michelfelder, S., Kohlschütter, J., Skorupa, A., Pfenning, S., Müller, O., Kleinschmidt, J.A., and Trepel, M. (2009). Successful expansion but not complete restriction of tropism of adeno-associated virus by in vivo biopanning of random virus display peptide libraries. *PLoS ONE* *4*, e5122.
- Körbelin, J., Sieber, T., Michelfelder, S., Lunding, L., Spies, E., Hunger, A., Alawi, M., Rapti, K., Indenbirken, D., Müller, O.J., et al. (2016). Pulmonary Targeting of Adeno-associated Viral Vectors by Next-generation Sequencing-guided Screening of Random Capsid Displayed Peptide Libraries. *Mol. Ther.* *24*, 1050–1061.
- Körbelin, J., and Trepel, M. (2017). How to Successfully Screen Random Adeno-Associated Virus Display Peptide Libraries In Vivo. *Hum. Gene Ther. Methods* *28*, 109–123.
- Dalkara, D., Byrne, L.C., Klimczak, R.R., Visel, M., Yin, L., Merigan, W.H., Flannery, J.G., and Schaffer, D.V. (2013). In vivo-directed evolution of a new adeno-associated virus for therapeutic outer retinal gene delivery from the vitreous. *Sci. Transl. Med.* *5*, 189ra76.
- Lisowski, L., Dane, A.P., Chu, K., Zhang, Y., Cunningham, S.C., Wilson, E.M., Nygaard, S., Grompe, M., Alexander, I.E., and Kay, M.A. (2014). Selection and evaluation of clinically relevant AAV variants in a xenograft liver model. *Nature* *506*, 382–386.
- Ojala, D.S., Sun, S., Santiago-Ortiz, J.L., Shapiro, M.G., Romero, P.A., and Schaffer, D.V. (2018). In Vivo Selection of a Computationally Designed SCHEMA AAV Library Yields a Novel Variant for Infection of Adult Neural Stem Cells in the SVZ. *Mol. Ther.* *26*, 304–319.
- Hanlon, K.S., Meltzer, J.C., Buzhdygan, T., Cheng, M.J., Sena-Esteves, M., Bennett, R.E., Sullivan, T.P., Razmpour, R., Gong, Y., Ng, C., et al. (2019). Selection of an Efficient AAV Vector for Robust CNS Transgene Expression. *Mol. Ther. Methods Clin. Dev.* *15*, 320–332.
- Deverman, B.E., Pravdo, P.L., Simpson, B.P., Kumar, S.R., Chan, K.Y., Banerjee, A., Wu, W.L., Yang, B., Huber, N., Pasca, S.P., and Gradinaru, V. (2016). Cre-dependent selection yields AAV variants for widespread gene transfer to the adult brain. *Nat. Biotechnol.* *34*, 204–209.
- Chan, K.Y., Jang, M.J., Yoo, B.B., Greenbaum, A., Ravi, N., Wu, W.L., Sánchez-Guardado, L., Lois, C., Mazmanian, S.K., Deverman, B.E., and Gradinaru, V. (2017). Engineered AAVs for efficient noninvasive gene delivery to the central and peripheral nervous systems. *Nat. Neurosci.* *20*, 1172–1179.
- Matsuzaki, Y., Konno, A., Mochizuki, R., Shinohara, Y., Nitta, K., Okada, Y., and Hirai, H. (2018). Intravenous administration of the adeno-associated virus-PHP.B capsid fails to upregulate transduction efficiency in the marmoset brain. *Neurosci. Lett.* *665*, 182–188.
- Hordeaux, J., Wang, Q., Katz, N., Buza, E.L., Bell, P., and Wilson, J.M. (2018). The Neurotropic Properties of AAV-PHP.B Are Limited to C57BL/6J Mice. *Mol. Ther.* *26*, 664–668.
- Liguore, W.A., Domire, J.S., Button, D., Wang, Y., Dufour, B.D., Srinivasan, S., and McBride, J.L. (2019). AAV-PHP.B Administration Results in a Differential Pattern of CNS Biodistribution in Non-human Primates Compared with Mice. *Mol. Ther.* *27*, 2018–2037.
- Stutika, C., Gogol-Döring, A., Botschen, L., Mietzsch, M., Weger, S., Feldkamp, M., Chen, W., and Heilbronn, R. (2015). A Comprehensive RNA Sequencing Analysis of the Adeno-Associated Virus (AAV) Type 2 Transcriptome Reveals Novel AAV Transcripts, Splice Variants, and Derived Proteins. *J. Virol.* *90*, 1278–1289.
- Mouw, M.B., and Pintel, D.J. (2000). Adeno-associated virus RNAs appear in a temporal order and their splicing is stimulated during coinfection with adenovirus. *J. Virol.* *74*, 9878–9888.
- Schoch, S., Cibelli, G., and Thiel, G. (1996). Neuron-specific Gene Expression of Synapsin I. *J. Biol. Chem.* *271*, 3317–3323.
- Lee, Y., Messing, A., Su, M., and Brenner, M. (2008). GFAP promoter elements required for region-specific and astrocyte-specific expression. *Glia* *56*, 481–493.
- DiMattia, M.A., Nam, H.-J., Van Vliet, K., Mitchell, M., Bennett, A., Gurda, B.L., McKenna, R., Olson, N.H., Sinkovits, R.S., Potter, M., et al. (2012). Structural insight into the unique properties of adeno-associated virus serotype 9. *J. Virol.* *86*, 6947–6958.

36. Deneke, J., Ziegelin, G., Lurz, R., and Lanka, E. (2000). The protelomerase of temperate Escherichia coli phage N15 has cleaving-joining activity. *Proc. Natl. Acad. Sci. U S A* 97, 7721–7726.
37. Zincarelli, C., Soltys, S., Rengo, G., and Rabinowitz, J.E. (2008). Analysis of AAV serotypes 1–9 mediated gene expression and tropism in mice after systemic injection. *Mol. Ther.* 16, 1073–1080.
38. Ravindra Kumar, S., Miles, T.F., Chen, X., Brown, D., Dobrev, T., Huang, Q., Ding, X., Luo, Y., Einarsson, P.H., Greenbaum, A., et al. (2020). Multiplexed Cre-dependent selection yields systemic AAVs for targeting distinct brain cell types. *Nat. Methods* 17, 541–550.
39. Hordeaux, J., Wang, Q., Katz, N., Buza, E.L., Bell, P., and Wilson, J.M. (2018). The Neurotropic Properties of AAV-PHP.B Are Limited to C57BL/6J Mice. *Mol. Ther.* 26, 664–668.
40. Hordeaux, J., Yuan, Y., Clark, P.M., Wang, Q., Martino, R.A., Sims, J.J., Bell, P., Raymond, A., Stanford, W.L., and Wilson, J.M. (2019). The GPI-Linked Protein LY6A Drives AAV-PHP.B Transport across the Blood-Brain Barrier. *Mol. Ther.* 27, 912–921.
41. Huang, Q., Chan, K.Y., Tobey, I.G., Chan, Y.A., Poterba, T., Boutros, C.L., Balazs, A.B., Daneman, R., Bloom, J.M., Seed, C., and Deverman, B.E. (2019). Delivering genes across the blood-brain barrier: LY6A, a novel cellular receptor for AAV-PHP.B capsids. *PLoS ONE* 14, e0225206.
42. Hordeaux, J., Yuan, Y., Clark, P.M., Wang, Q., Martino, R.A., Sims, J.J., Bell, P., Raymond, A., Stanford, W.L., and Wilson, J.M. (2019). The GPI-Linked Protein LY6A Drives AAV-PHP.B Transport across the Blood-Brain Barrier. *Mol. Ther.* 27, 912–921.
43. Wang, Z., Ma, H.I., Li, J., Sun, L., Zhang, J., and Xiao, X. (2003). Rapid and highly efficient transduction by double-stranded adeno-associated virus vectors in vitro and in vivo. *Gene Ther.* 10, 2105–2111.
44. Körbelin, J., Dogbevia, G., Michelfelder, S., Ridder, D.A., Hunger, A., Wenzel, J., Seismann, H., Lampe, M., Bannach, J., Pasparakis, M., et al. (2016). A brain microvasculature endothelial cell-specific viral vector with the potential to treat neurovascular and neurological diseases. *EMBO Mol. Med.* 8, 609–625.
45. Taschenberger, G., Tereshchenko, J., and Kügler, S. (2017). A MicroRNA124 Target Sequence Restores Astrocyte Specificity of gfaABC1D-Driven Transgene Expression in AAV-Mediated Gene Transfer. *Mol. Ther. Nucleic Acids* 8, 13–25.
46. Powell, S.K., Samulski, R.J., and McCown, T.J. (2020). AAV Capsid-Promoter Interactions Determine CNS Cell-Selective Gene Expression In Vivo. *Mol. Ther.* 28, 1373–1380.
47. Crosson, S.M., Dib, P., Smith, J.K., and Zolotukhin, S. (2018). Helper-free Production of Laboratory Grade AAV and Purification by Iodixanol Density Gradient Centrifugation. *Mol. Ther. Methods Clin. Dev.* 10, 1–7.
48. Zorita, E., Cuscó, P., and Filion, G.J. (2015). Starcode: sequence clustering based on all-pairs search. *Bioinformatics* 31, 1913–1919.
49. Langmead, B., Trapnell, C., Pop, M., and Salzberg, S.L. (2009). Ultrafast and memory-efficient alignment of short DNA sequences to the human genome. *Genome Biol.* 10, R25.
50. van der Loo, M.P.J. (2014). The stringdist package for approximate string matching. *R J.* 6, 111–122.

OMTM, Volume 20

Supplemental Information

Rapid evolution of blood-brain- barrier-penetrating AAV capsids by RNA-driven biopanning

Mathieu Nonnenmacher, Wei Wang, Matthew A. Child, Xiao-Qin Ren, Carol Huang, Amy Zhen Ren, Jenna Tocci, Qingmin Chen, Kelsey Bittner, Katherine Tyson, Nilesh Pande, Charlotte Hiu-Yan Chung, Steven M. Paul, and Jay Hou

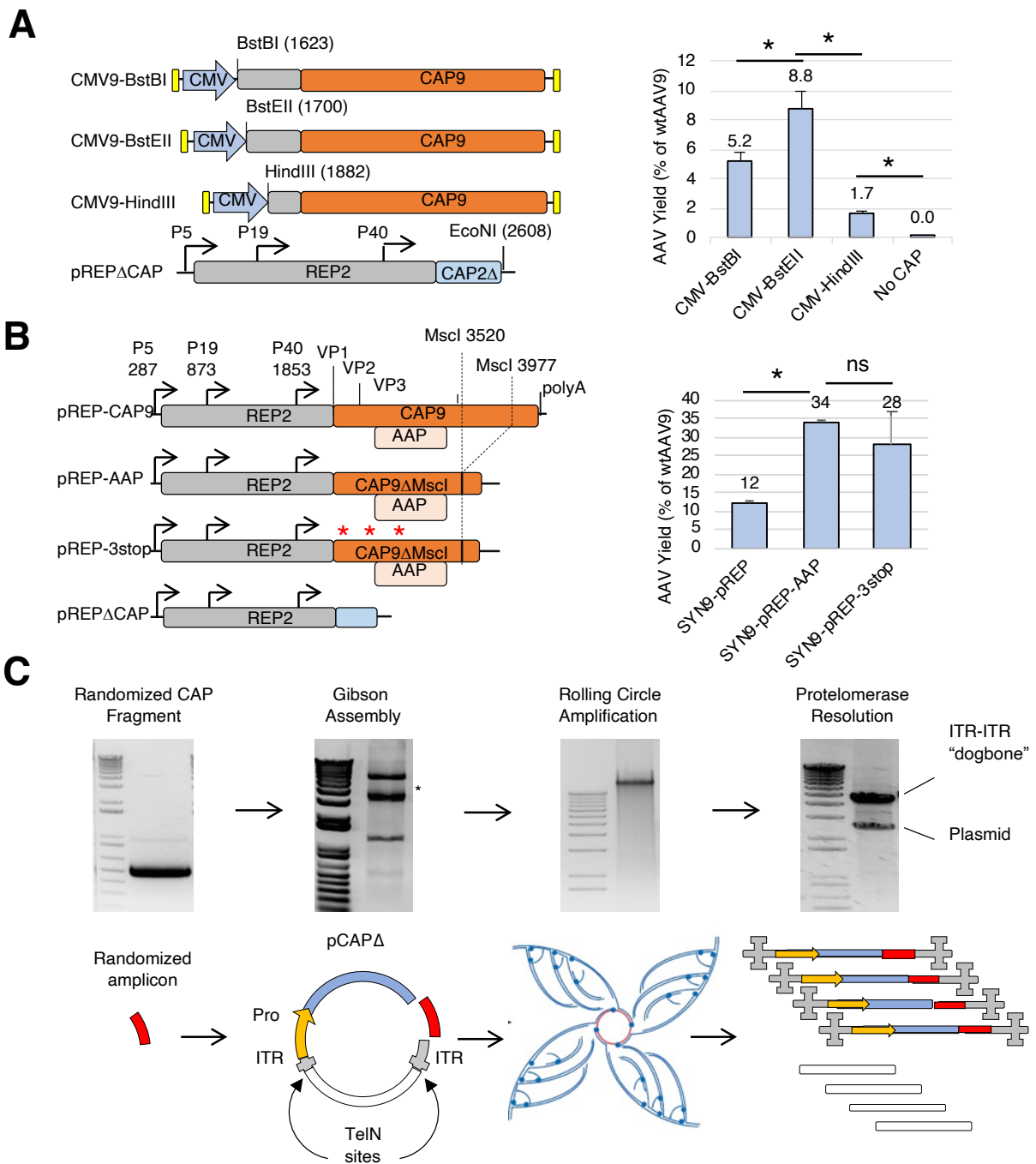


Figure S1 . TRACER library design and optimization.

(A) Identification of the minimal *cis* sequences necessary for efficient AAV production. Variable 5' REP sequences from ITR-REP-CAP9-ITR wild-type vector were replaced by a CMV promoter. The REP protein was provided in *trans* by the pREP Δ CAP vector (depicted). Genome titers obtained with each construct are shown on the right bar graph. Values indicate mean \pm SD (n=3) percent of wtAAV9 titers. *p < 0.05 (unpaired t test). (B) Optimization of REP vector. Top: map of the parent REP2CAP9 construct showing the position of AAV promoters, CAP ORF start codons and the MscI truncations. The pREP-3stop vector contains nonsense mutations downstream of each capsid ORF start codon (red asterisks). Each REP plasmid was used to produce an ITR-SYN-CAP9-ITR vector (not pictured). The bar graph represents the mean \pm SD (n=3) percentage of wtAAV9 genomic titers. *p < 0.05 (unpaired t test); ns, not significant. (C) High-diversity library generation by cloning-free rolling circle amplification. See materials and methods for details.

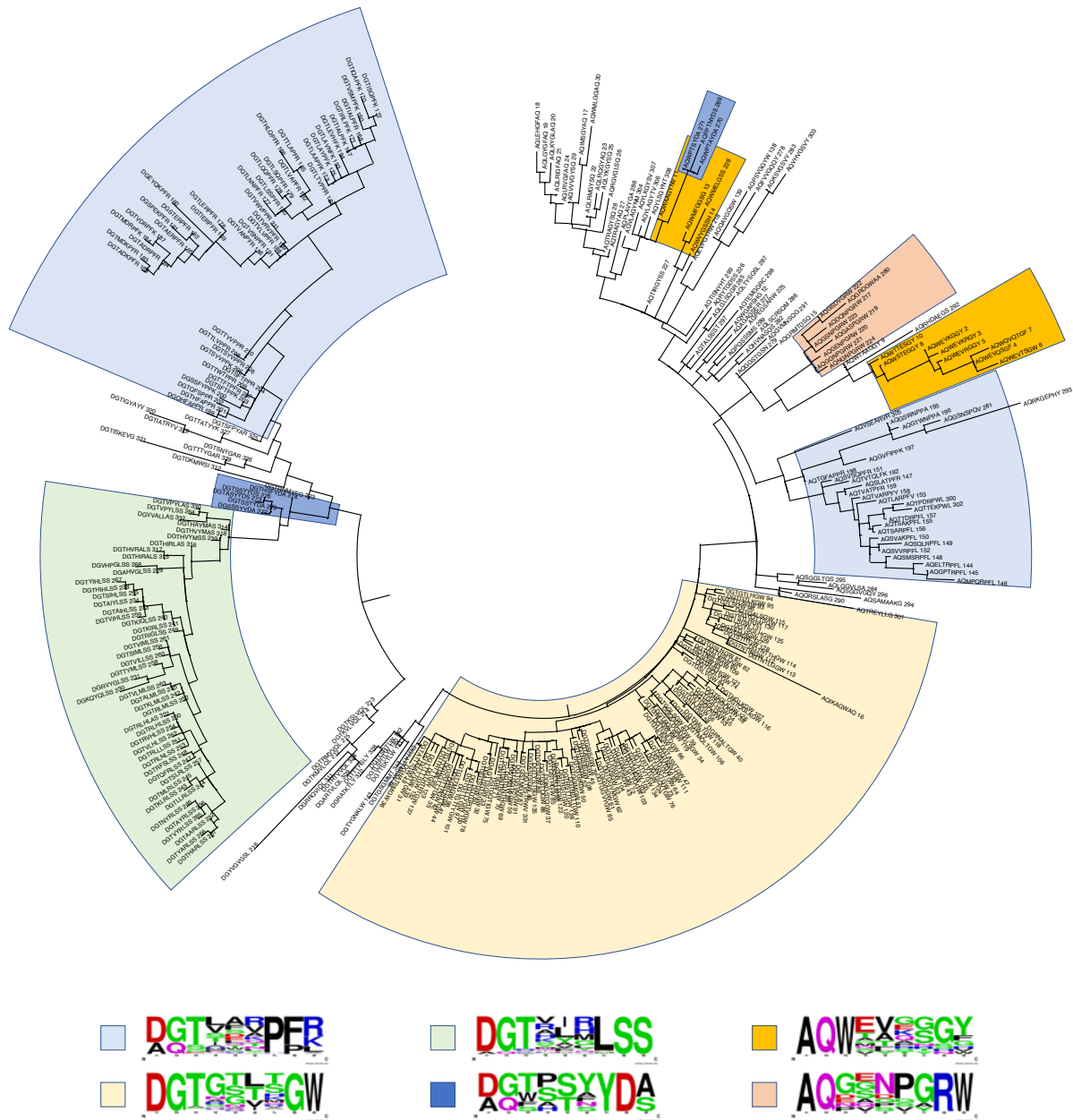


Figure S2. Phylogenetic Analysis of 330 Top BBB-Crossing Variants.

Maximum-likelihood phylogeny relating 330 top variants from mouse brain RNA enrichment analysis. Phylogenetic tree of 9-mer variable peptide inserts was constructed using MEGAX. Clusters of peptide sequences sharing high homology are highlighted. Frequency plots of each major cluster are shown at the bottom. The DGTxxxPF[+] consensus motif is shared with PHP.B and PHP.eB capsids and referred to as “PHP-like” in the main text.

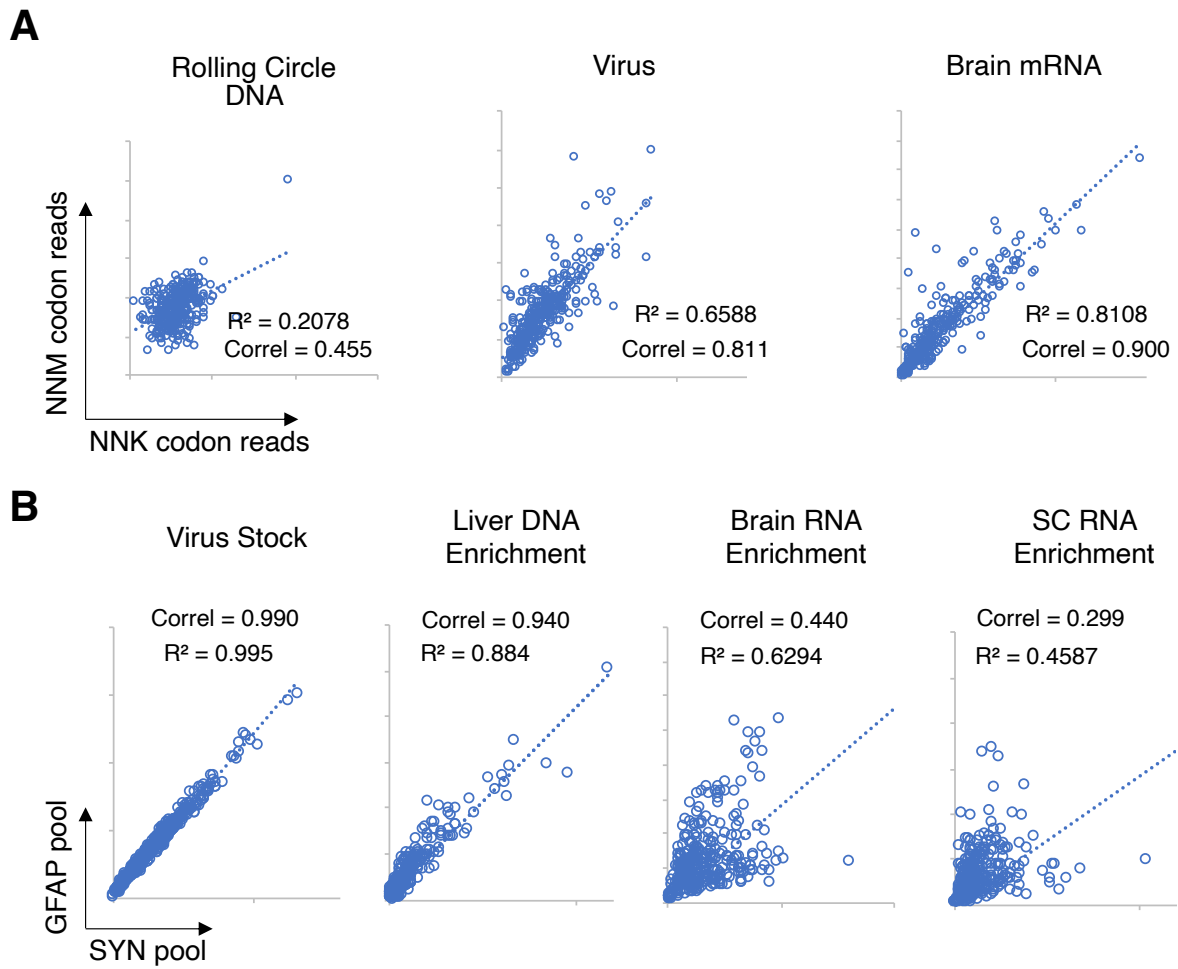


Figure S3 . Correlation analysis of synthetic pooled library.

(A) Codon variant correlation. Scatter plots indicate normalized NGS reads from NNM codon variants (Y axis) and NNK codon variants (X axis) of each capsid mutant in the Rolling circle DNA (left), the virus preparation (middle) and the brain mRNA samples recovered from C57Bl/6 mice (right). Both axes are in linear scale. (B) Correlation analysis of SYN- and GFAP-driven capsid pools in the virus stock, liver DNA, brain RNA and spinal cord RNA. Both axes are in linear scale. Note the high correlation in liver DNA suggesting consistency of both libraries.

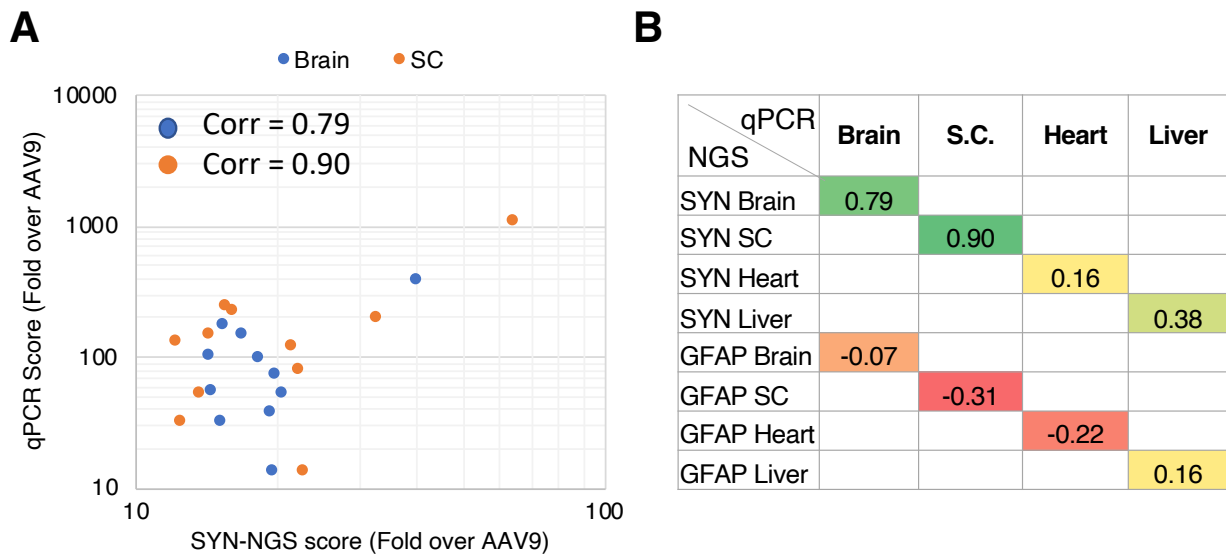


Figure S4. Correlation analysis between multiplexed NGS analysis and individual capsid qPCR quantitation. (A) Scatter plot showing the score of each capsid variant as measured by multiplexed brain RNA enrichment (X axis) or individual qPCR RNA quantitation (Y axis) in the brain (blue dots) and spinal cord (orange dots). Values from both assays are normalized to AAV9 for consistency. The correlation coefficients are indicated. (B) Correlation coefficients between qPCR data (rows) and SYN- or GFAP-driven NGS data (columns) of 12 capsids (10 candidates + PHP.eB + AAV9) in the brain, spinal cord, heart and liver. Note the high correlation coefficient obtained with the SYN-driven TRACER data.

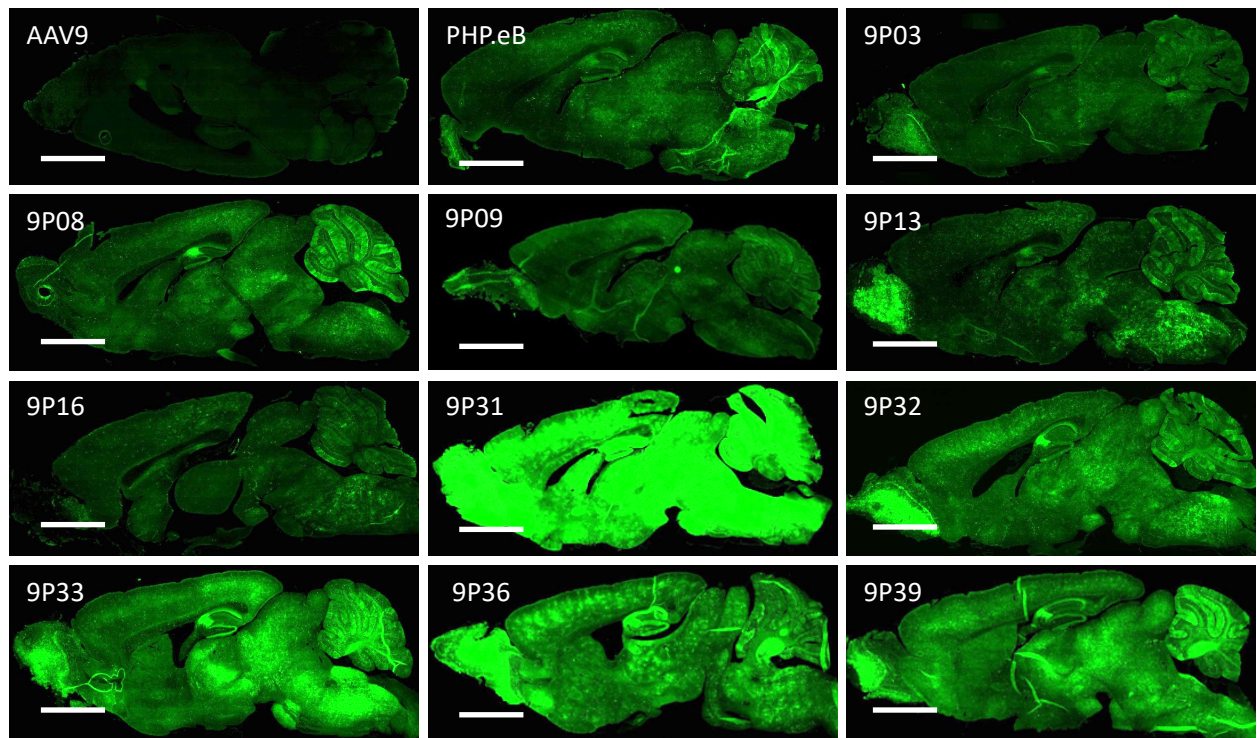
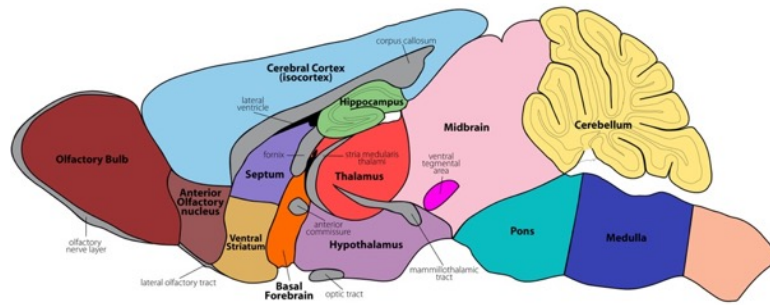
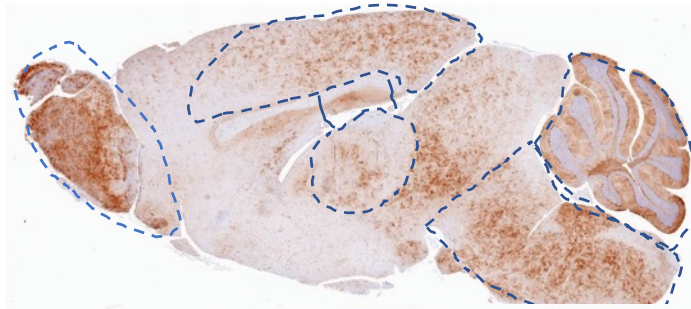


Figure S5. General brain transduction profile of TRACER capsid candidates after intravascular infusion in adult mice.

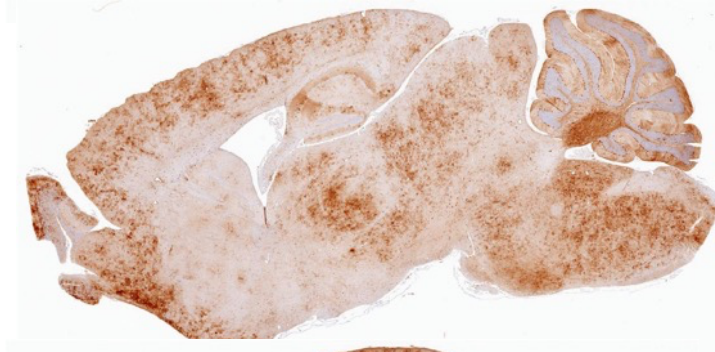
Native EGFP fluorescence was observed in sagittal cryosections from the brain of adult C57Bl/6 mice 28 days after dosing with 4×10^{11} VG per mouse. Bar: 2 mm.



9P13



9P16



9P31



9P33



Figure S6. Representative pattern of transduction by TRACER capsids in mouse brain.

EGFP IHC from mouse brains 28 days after intravascular infusion with 9P13, 9P31 and 9P33 capsids (4e11VG per mouse). Major brain regions are depicted in the top diagram (image from <http://www.gensat.org>).

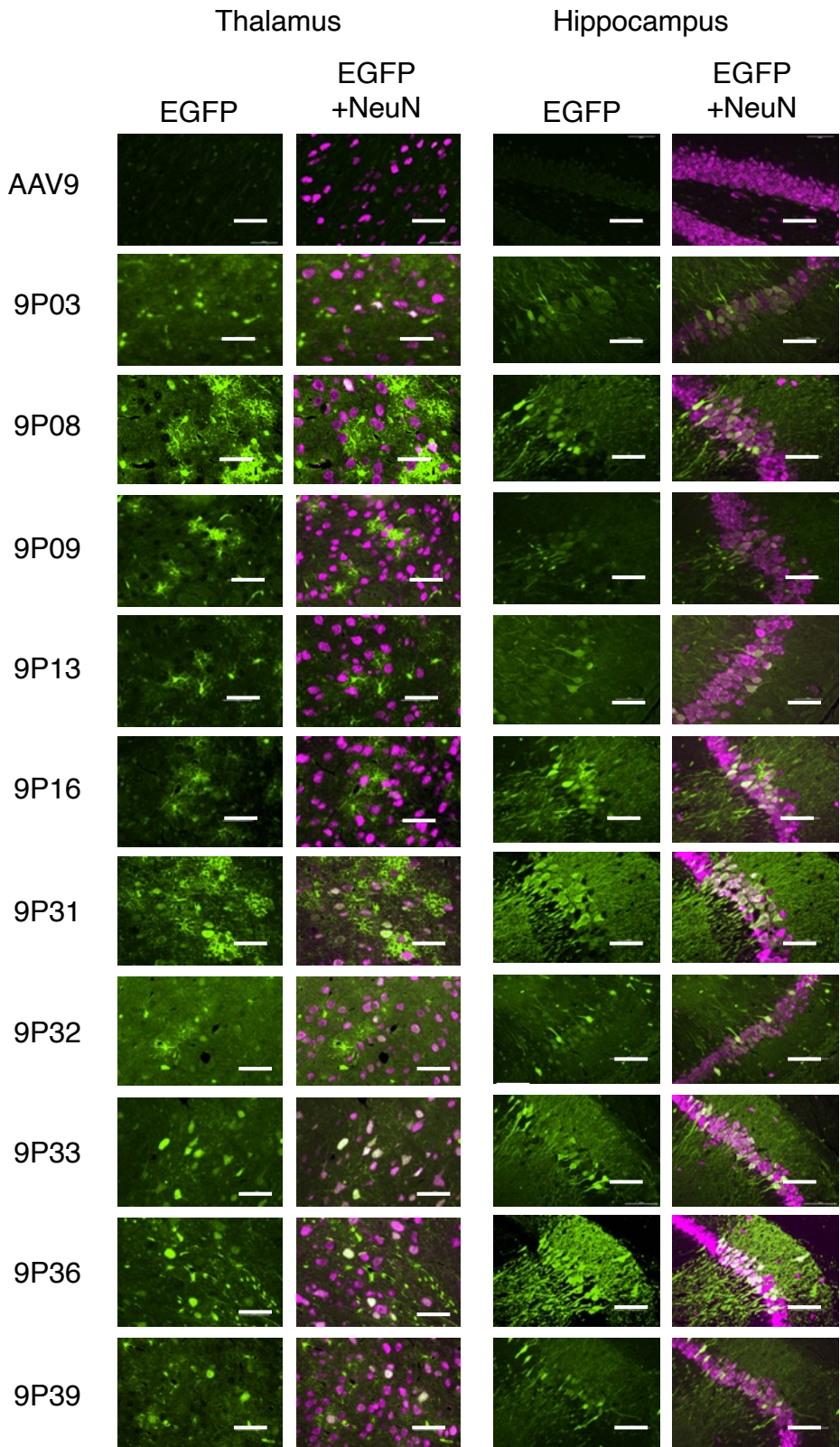


Figure S7. Neuron transduction by TRACER capsids in mouse Thalamus and Hippocampus.
 Co-immunostaining of EGFP (green) and NeuN (magenta) in the brain of mice one month after intravenous dosing with 4×10^{11} VG of engineered capsids. Bar: 50 μ m.

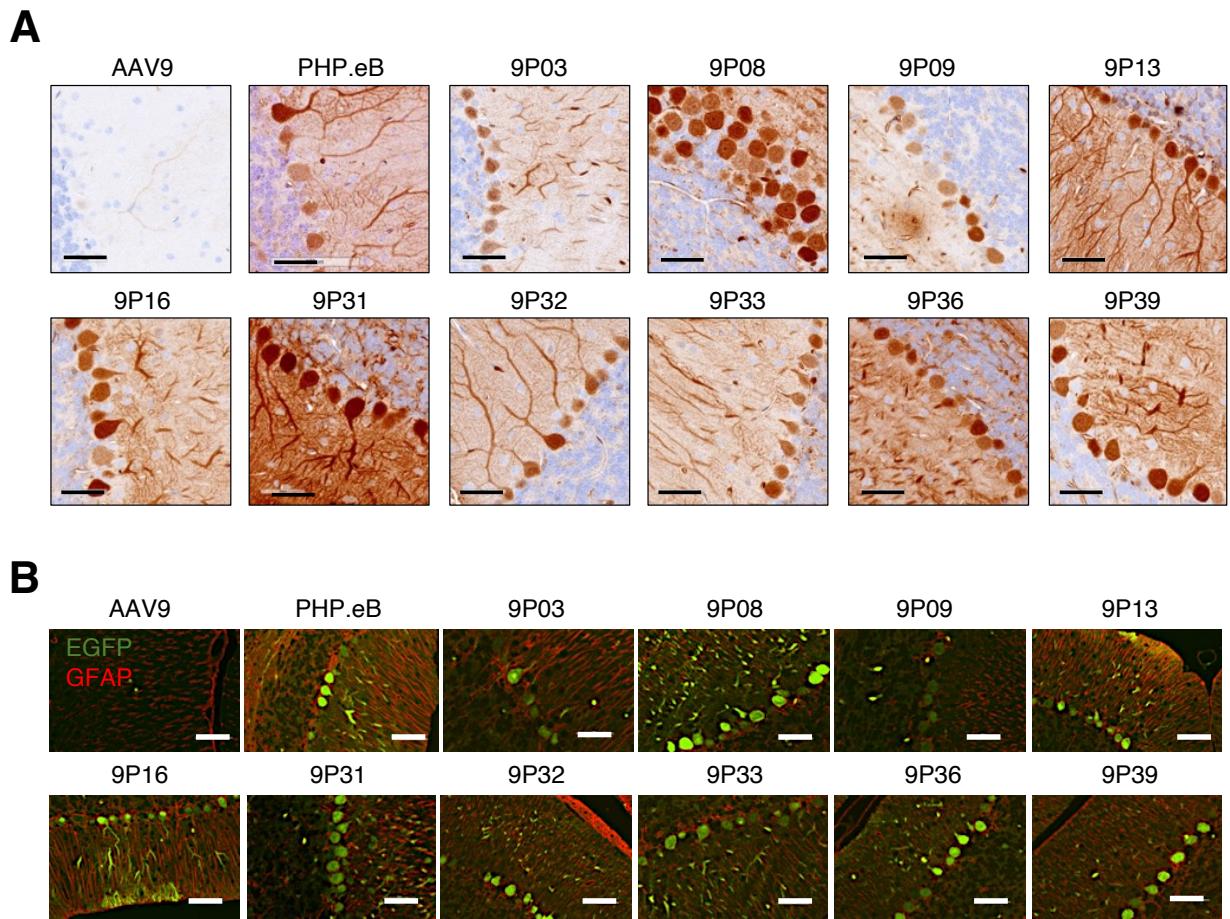


Figure S8. Transduction by TRACER capsids in mouse cerebellum.

(A) Detail of EGFP immunostaining in mouse cerebellum 28 days after intravascular infusion (4×10^{11} VG per mouse).

(B) Co-immunostaining of EGFP (green) and GFAP (red) in the cerebellum. Bar, 50 μ m.

Supplemental Table 1. Primers and probes used in this study

Primer name	Primer sequence (5' to 3')
9L8-F24	CAAGTGGCCACAAACCACCAGAGTgcccaanNNKNNKNNKNNKNNKNNKNNKGCACAGGCGCAGACCGGCTG
9DGL8-F24	CAAGTGGCCACAAACCACCAGAGTgatggcNNKNNKNNKNNKNNKNNKNNKGCACAGGCGCAGACCGGCTG
9DRTL8-F24	CAAGTGGCCACAAACCACCAGAGTgatggcaccNNKNNKNNKNNKNNKNNKNNKGCACAGGCGCAGACCGGCTG
CAP9-L8F	CAAGTGGCCACAAACCACCAGAGT
CAP9-StopR23	CGGTTTATTGATTAACAATCGATTACAGATTACGAGTCAGGTATC
CAP9L8 gBlock ^a ΔBamHI ΔAfeI	GCACAGGCGCAGACCGGCTGGGTTCAAACCAAGGAATACTTCCGGGTATGGTTTGGCAGGACAGAGATGTGTACCTGCAAGGACC CATTTGGGCCAAAATTCCTCACACGGACGGCAACTTTCACCTTTCCTCCGTGATGGGAGGGTTTGGAAATGAAGCACCCGCCTCCTC AGATCCTCATCAAAAACACACCTGTACCTGCcGATCCTCCAACGGCCTTCAACAAGGACAAGCTGAACTCTTTCATCACCCAGTAT TCTACTGGCCAAGTCAGCGTGGAGATCGAGTGGGAGCTGCAGAAGAAAAACAGCAAGCGgTGGAACCCGGAGATCCAGTACACTTC CAACTATTACAAGTCTAATAATGTTGAATTTGCTGTTAATACTGAAGGTGTATATAGTGAACCCCGCCCATTTGGCACAGATAACC TGACTCGTAATCTGTAA
SpliceF6 ^b	GTGCCAAGAGTGAC/CTCCTG
CAP-RT	GAAACGAATTAACCGTTTATTGATTAACAATCGATTA
9*NGS-F4N	AATGATACGGCGACCACCGAGATCTACACTCTTTCCCTACACGACGCTCTTCCGATCTNNNNTTGGCCACAAACCACCAGAGT
9*NGS-F3N	AATGATACGGCGACCACCGAGATCTACACTCTTTCCCTACACGACGCTCTTCCGATCTNNNNTTGGCCACAAACCACCAGAGT
9*NGS-F2N	AATGATACGGCGACCACCGAGATCTACACTCTTTCCCTACACGACGCTCTTCCGATCTNNNTGGCCACAAACCACCAGAGT
9*NGS-R ^c	CAAGCAGAAGACGGCATAACGAGAT (nnnnnn)GTGACTGGAGTTCAGACGCTGTCTCTTCCGATCTTGGTTTGAACCCAGCCGGT
REP-Fwd2	TTTCCGGTGGGCAAAGG
REP-Rev2	GCTCACTTATATCTGCGTCACT
REP-Probe	ACGTGGTTGAGGTGGAGCATGAAT
GloX4-F	GGGAACGGTGCATTGGAA
GloX4-R	GATGGCCAGCACACAG
GloX4-Probe ^b	AAGAGTGAC/CTCCTGGGCAACG
EGFP	Life Technologies Mr04329676_mr Taqman set
Mouse TBP	Life Technologies Mm01277042_m1 Taqman set
Human GAPDH	Life Technologies Hs01922876_u1 Taqman set
Mouse TERT	Life Technologies Mm00653609_cn Taqman set

^aSilent mutations have been introduced to remove BamHI and AfeI sites

^bSpecific for CMV-Globin Exon-Exon junction, does not work on DNA

^cBracketed 6-mer represents the site if insertion of illumina TruSeq index for multiplexing

VECTOR SEQUENCES

TRACER-SYN-9-BsrGI (6827bp)

Features:

17-161: Left ITR
207-763: Human Synapsin 1 promoter
784-1349: CMV-Globin hybrid intron
1372-1857: AAV2 REP C-terminal sequence
1875-3631: AAV9 CAP Fragment
3632-3637: BsrGI restriction site
3762-3906: Right ITR
4008-4063: TelN recognition sequence
4718-5575: Ampicillin Resistance
6577-6632: TelN recognition sequence

```
CCTTAATTAGGCTAGCTTGGCCACTCCCTCTCTGCGCGCTCGCTCGCTCACTGAGGCCGGGGCACCACAAAGGTCGCCC
GACGCCCGGGCTTTGCCCGGGCGGCCTCAGTGAGCGAGCGAGCGCGCAGAGAGGGAGTGGCCAACCTCCATCACTAGG
GGTTCCTGGAGGGGTGGAGTCGTGACGATATCCATGCGTGCACATAACCGCTTAGTATCTGCAGAGGGCCCTGCCTA
TGAGTGCAAGTGGGTTTTAGGACCAGGATGAGGCGGGGTGGGGGTGCCTACCTGACGACCGACCCCGACCCACTGGA
CAAGCACCCAACCCCAATTCCCAAAATTGCGCATCCCTATCAGAGAGGGGGAGGGGAAACAGGATGCGGCGAGGGCG
CGTGCGCACTGCCAGCTTCAGCACCGCGGACAGTGCCTTCGCCCCCGCCTGGCGGCGCGGCCACCGCCGCTCAGC
ACTGAAGGCGCGCTGACGTCCTCGCCGGTCCCCGCAAACCTCCCTTCCCGGCCACCTTGGTTCGCGTCCGCGCCGC
CGCCGGCCAGCCGGACCGCACCACGCGAGGCGCGAGATAGGGGGGCACGGGCGCGACCATCTGCGCTGCGGCGCCG
GCGACTCAGCGCTGCCTCAGTCTGCGGTGGGCAGCGGAGGAGTCGTGTCTGCTGAGAGCGCAGCTGTGCTCCTGG
GCACCGCGCAGTCCGCCCCCGGGTCTCTGGCCAGACCACCCCTAGGACCCCTGCCCAAGTCGCAGCCAAAGCTTC
GTTTAGTGAACCGTCAGATCGCCTGGAGACGCCATCCACGCTGTTTTGACCTCCATAGAAGACACCGGGACCGATCC
AGCCTCCGCGGATTCGAATCCCGCCGGGAACGGTGCATTGGAACGCGGATTCGCCGTGCCAAGAGTGACGTAAGTA
CCGCTATAGAGTCTATAGGCCACAAAAAATGCTTCTCTTTTAATATACTTTTTTGTATTATCTTATTTCTAATA
CTTTCCCTAATCTCTTTCTTTTCAGGGCAATAATGATACAATGATCATGCCTCTTTGCACCATCTAAAGAATAACA
GTGATAATTTCTGGGTTAAGGCAATAGCAATATTTCTGCATATAAAATATTTCTGCATATAAAATGTAAGTATGTA
GAGGTTTCATATTGCTAATAGCAGCTACAATCCAGCTACCATTCTGCTTTTTATTTTATGGTTGGGATAAGGCTGGAT
TATTCTGAGTCCAAGCTAGGCCCTTTTGCTAATCATGTTTCATACCTCTTATCTTCTCCACAGCTCCTGGGCAACG
TGCTGGTCTGTGTGCTGGCCCATCACTTTGGCAAAGAATTGGGATTCGAACCGGTCGCCACCGGTCACCAAGCAGGA
AGTCAAAGACTTTTTCCGGTGGGCAAAGGATCACGTGGTTGAGGTGGAGCATGAATTCTACGTCAAAAAGGGTGGAG
CCAAGAAAAGACCCGCCCCAGTGACGCAGATATAAGTGAGCCCAAACGGGTGCGCGAGTCAGTTGCGCAGCCATCG
ACGTGACGCGGAAGCTTCGATCAACTACGCGGACAGGTACCAAAACAAATGTTCTCGTCACGTGGGCATGAATCT
GATGCTGTTTTCCCTGCAGACAATGCGAGAGACTGAATCAGAATTCAAATATCTGCTTCACTCACGGTGTCAAAGACT
GTTTAGAGTGCTTTCCCGTGTGAGAATCTCAACCCGTTTCTGTGCTCAAAAAGGCGTATCAGAAACTGTGCTACATT
CATCACATCATGGGAAAGGTGCCAGACGCTTGCACTGCTTGGCAGCTGGTCAATGTGGACTTGGATGACTGTGTTTC
TGAACAATAAATGACTTAAACCAGGTATGGCTGCCGATGGTTATCTTCCAGATTGGCTCGAGGACAACCTTAGTGAA
GGAATTCGCGAGTGGTGGGCTTTGAAACCTGGAGCCCTCAACCCAAGGCAAAATCAACAACATCAAGACAACGCTCG
AGGTCTTGTGCTTCCGGTTACAAATACCTTGGACCCGGCAACGACTCGACAAGGGGGAGCCGGTCAACGCAGCAG
ACGCGGCGGCCCTCGAGCAGCACAAGGCCTACGACCAGCAGCTCAAGGCCGGAGACAACCCGTACCTCAAGTACAAC
CACGCCGACGCCGAGTTCCAGGAGCGGCTCAAAGAAGATACGTCTTTTGGGGCAACCTCGGGCGAGCAGTCTTCCA
GGCCAAAAGAGGCTTCTTGAACCTCTTGGTCTGGTTGAGGAAGCGGCTAAGACGGCTCCTGGAAAGAAGAGGCCTG
TAGAGCAGTCTCCTCAGGAACCGGACTCCTCCGCGGGTATTGGCAAATCGGGTGCACAGCCCGCTAAAAAGAGACTC
AATTTCCGTCAGACTGGCGACACAGAGTCAGTCCAGACCCTCAACCAATCGGAGAACCTCCCGCAGCCCCCTCAGG
TGTGGGATCTCTTACAATGGCTTCCAGGTGGTGGCGCACCAGTGGCAGACAATAACGAAGGTGCCGATGGAGTGGGTA
GTTCTCAGGAAATGGCATTGCGATTCCCAATGGCTGGGGGACAGAGTCATCACCACCAGCACCCGAACCTGGGCC
CTGCCACCTACAACAATCACCTCTACAAGCAAATCTCCAACAGCACATCTGGAGGATCTTCAAATGACAACGCCTA
CTTCGGCTACAGCACCCCTGGGGTATTTTACTTCAACAGATTCCACTGCCACTTCTCACCACGTGACTGGCAGC
GACTCATCAACAACAACCTGGGGATTCGGCCTAAGCGACTCAACTTCAAGCTCTTCAACATTCAGGTCAAAGAGGTT
ACGGACAACAATGGAGTCAAGACCATCGCAATAACCTTACCAGCAGCTCCAGGCTTTCACGGACTCAGACTATCA
GCTCCCGTACGTGCTCGGGTCCGCTCACGAGGGTCCCTCCCGCGTTCAGCGGACGTTTTTCAATGATTTCTCAGT
ACGGGTATCTGACGCTTAATGATGGAAGCCAGGCCGTGGGTCGTTTCGTCCTTTTACTGCCTGGAATATTTCCCGTCG
CAAATGCTAAGAACGGGTAACAACCTTCCAGTTCAGCTACGAGTTTGGAGAAGCTACCTTTCCATAGCAGCTACGCTCA
CAGCCAAAGCCTGGACCGACTAATGAATCCACTCATCGACCAATACTTGTACTATCTCTCAAAGACTATTAACGGTT
CTGGACAGAATCAACAACGCTAAAATTCAGTGTGGCCGGACCCAGCAACATGGCTGTCCAGGGAAGAAACTACATA
CCTGGACCCAGCTACCGACAACAACGTGTCTCAACCACTGTGACTCAAAAACAACAACAGCGAATTTGCTTGGCCTGG
```


AGCTTCTTCTTGGGCTCTCAATGGACGTAATAGCTTGTATGAATCCTGGACCTGCTATGGCCAGCCACAAAGAAGGAG
AGGACCGTTTTCTTTCCCTTTGTCTGGATCTTTAATTTTTGGCAAACAAGGAAGCTGGAAGAGACAACGTGGATGCGGAC
AAAGTCATGATAACCAACGAAGAAGAAATTAATACTACTAACCCGGTAGCAACGGAGTCCCTATGGACAAGTGGCCAC
AAACCACCAGAGTGTACAATCGATTGTTAATCAATAAACCGTTAATTCGTTTCAGTTGAACTTTGGTCTCTGCGTAT
TTCTTTCTTATCTAGTTTCCATGGCTACGTAGATAAGTAGCATGGCGGGTTAATCATTAACTACAAGGAACCCCTAG
TGATGGAGTTGGCCACTCCCTCTCTGCGCGCTCGCTCGCTCACTGAGGCCGGGCGACCAAGGTCGCCCCGACGCCCG
GGCTTTGCCCGGGCGGCTCAGTGAGCGAGCGAGCGCGAGAGAGGGAGTGGCCAAATGCAATTAACTGGCCGTC
GTTTTACAACGTCGTGACTGGGAAAACCTGGCGTTACCCAATTAATCGCCTTGCAGCACATCCCCCTTTGCGCAG
CTGTATCAGCACACAATTGCCATTATACGCGCGTATAATGGACTATTGTGTGCTGATAGCGTAATAGCGAAGAGGC
CCGCACCGATCGCCCTTCCCAACAGTTGCGCAGCCTGAATGGCGAATGGGACGCGCCCTGTAGCGGCGCATTAAAGCG
CGGCGGGTGTGGTGGTTACGCGCAGCGTGACCGCTACACTTGCCAGCGCCCTAGCGCCCGCTCCTTTGCGTTTCTTC
CCTTCTTTCTCGCCACGTTTCGCCGGCTTTCCCGTCAAGCTCTAAATCGGGGGCTCCCTTTAGGGTTCCGATTTAG
TGCTTTACGGCACCTCGACCCCAAAAACTTGATTAGGGTGTATGGTTTACGTAAGTGGGCCATCGCCCTGATAGACGG
TTTTTTGCGCCTTTGACGTTGGAGTCCACGTTCTTTAATAGTGGACTCTTGTTCAAAATGGAACAACACTCAACCCT
ATCTCGGTCTATTCTTTTGTATTTATAAGGGATTTTGGCGATTTGCGCCTATTGGTTAAAAAATGAGCTGATTTAACA
AAAATTTAACGCGAATTTTAAACAAAATATTAACGCTTACAATTTAGGTGGCACTTTTCGGGAAATGTGCGCGGAAC
CCCTATTTGTTTTATTTTTCTAAATACATTTCAAATATGTATCCGCTCATGAGACAATAACCCTGATAAATGCTTCAAT
AATATTGAAAAGGAAGAGTATGAGTATTCAACATTTCCGTGTCGCCCTTATTCCCTTTTTTTGCGGCATTTTGCCTT
CCTGTTTTTTGCTCACCCAGAAACGCTGGTGAAAGTAAAAGATGCTGAAGATCAGTTGGGTGCACGAGTGGGTTACAT
CGAAGTGGATCTCAACAGCGGTAAGATCCTTGAGAGTTTTTCGCCCGAAGAACGTTTTTCCAATGATGAGCACTTTTA
AAGTTCTGCTATGTGGCGCGGTATTATCCCGTATTGACGCCGGGCAAGAGCAACTCGGTGCGCGCATAACTATTCT
CAGAATGACTTGGTTGAGTACTCACAGTCACAGAAAAGCATCTTACGGATGGCATGACAGTAAGAGAATTATGCAG
TGCTGCCATAACCATGAGTGATAACACTGCGGCCAACTTACTTCTGACAACGATCGGAGGACCGAAGGAGCTAACCG
CTTTTTTGACAACATGGGGGATCATGTAACCTCGCCTTGATCGTTGGGAACCGGAGCTGAATGAAGCCATAACAAAC
GACGAGCGTGACACCACGATGCCTGTAGCAATGGCAACAACGTTGCGCAAACTATTAACTGGCGAACTACTTACTCT
AGCTTCCCGGCAACAATTAATAGACTGGATGGAGGCGGATAAAGTTGCAGGACCCTTCTGCGCTCGGCCCTTCCGG
CTGGCTGGTTTTATTGCTGATAAATCTGGAGCCGGTGAGCGTGGGTCTCGCGGTATCATTGCAGCACTGGGGCCAGAT
GGTAAGCCCTCCCGTATCGTAGTTATCTACACGACGGGGAGTCAGGCAACTATGGATGAACGAAATAGACAGATCGC
TGAGATAGGTGCCCTCACTGATTAAGCATTGGTAACCTGTCAGACCAAGTTTACTCATATATACTTTAGATTGATTAA
AACTTCATTTTTAATTTAAAAGGATCTAGGTGAAGATCCTTTTTGATAATCTCATGACCAAAATCCCTTAACGTGAG
TTTTTCGTTCCACTGAGCGTCAGACCCCGTAGAAAAGATCAAAGGATCTTCTTGAGATCCTTTTTTTTTCTGCGGTAAT
CTGCTGCTTGCAACAAAAAAACCACCGCTACCAGCGGTGGTTTTGTTTTGCCGGATCAAGAGCTACCAACTCTTTTTTC
CGAAGGTAACCTGGCTTCAGCAGAGCGCAGATACCAAATACTGTTCTTCTAGTGTAGCCGTAGTTAGGCCACCACTTC
AAGAACTCTGTAGCACCGCTACATACTCGCTCTGCTAATCCTGTTACCAGTGGCTGCTGCCAGTGGCGATAAGTC
GTGTCTTACCGGGTTGGACTCAAGACGATAGTTACCGGATAAGGCGCAGCGGTGCGGCTGAACGGGGGGTTCTGTGCA
CACAGCCCAGCTTGGAGCGAACGACCTACACCGAACTGAGATACCTACAGCGTGAGCTATGAGAAAGCGCCACGCTT
CCCGAAGGGGAGAAAGGCGGACAGGTATCCGGTAAGCGGCAGGGTCGGAACAGGAGAGCGCACGAGGGAGCTTCCAGG
GGGAAACGCCTGGTATCTTTATAGTCTGTGCGGTTTTGCCACCTCTGACTTGAGCGTTCGATTTTTTGTGATGCTCGT
CAGGGGGGCGGAGCCTATGGAAAAACGCCAGCAACGCGGCCTTTTTACGGTTCTGGCCTTTTGTGCTGGCCTTTTGTCT
CACATGTTCTTTCTGCGTTATCCCCTGATTCTGTGGATAACCGTATTACCGCCTTTGAGTGGCTGATACCGCTCG
CCGACGCCAAGCAGCCGAGCGCAGCGAGTCAGTGAGCGAGGAAGCGGAAGAGCGCCCAATACGCAAACCGCCTCC
CCGCGCTTGGCCGATTCATTAATGTCTAGATATCAGCACACAATAGTCCATTATACGCGCGTATAATGGGCAATTG
TGTGCTGATACAGCTGGCAGCAGAGTTTTCCCGACTGGAAAGCGGGCAGTGAGCGCAACGCAATTAATGTGAGTTAG
CTCACTCATTAGGCACCCAGGCTTTACACTTTATGCTTCCGGCTCGTATGTTGTGTGGAATTTGTGAGCGGATAACA
ATTTTACACAGGAAACAGCTATGACCATGATTACGCCAGATTTAATTAAGG

TRACER-GFAP-9-BsrGI (6827bp)

Features:

- 17-161: Left ITR
- 207-905: GFAbclD promoter
- 926-1491: CMV-Globin hybrid intron
- 1514-2000: AAV2 REP C-terminal sequence
- 2017-3773: AAV9 CAP Fragment
- 3774-3779: BsrGI restriction site
- 3904-4048: Right ITR
- 4150-4205: TelN recognition sequence
- 4860-5720: Ampicillin Resistance
- 6719-6774: TelN recognition sequence

CCTTAATTAGGCTAGCTTGGCCACTCCCTCTCTGCGCGCTCGCTCGCTCACTGAGGCCGGGGCACCAAAGGTCGCCC
GACGCCCCGGGCTTTGCCCGGGCGGCTCAGTGAGCGAGCGAGCGCGCAGAGAGGGAGTGGCCAACCTCCATCACTAGG
GGTTCCTGGAGGGGTGGAGTCTGTGACGATATCCATGCGTGCACATAACCGGTGATCTAACATATCTGGTGTGGAGT
AGCGGACGCTGCTATGACAGAGGCTCGGGGGCCTGAGCTGGCTCTGTGAGCTGGGGAGGAGGCAGACAGCCAGGCT
TGTCTGCAAGCAGACCTGGCAGCATTGGGCTGGCCGCCCCAGGGCTCCTCTTCATGCCCAGTGAATGACTCACC
TTGGCACAGACACAATGTTCCGGGTGGGCACAGTGCCTGCTTCCCGCCGACCCAGCCCCCTCAAATGCCTTCCG
AGAAGCCCATTGAGCAGGGGGCTTGCATTGCACCCAGCCTGACAGCCTGGCATCTTGGGATAAAAGCAGCACAGCC
CCCTAGGGGCTGCCCTTGTGTGGCGCCACCGCGGTGGAGAACAAGGCTCTATTTCAGCCTGTGCCAGGAAAGG
GGATCAGGGGATGCCCAGGCATGGACAGTGGGTGGCAGGGGGGAGAGGAGGGCTGTCTGCTTCCAGAAGTCCAAG
GACACAAATGGGTGAGGGGAGAGCTCTCCCATAGCTGGGCTGCGGCCAACCCACCCCTCAGGCTATGCCAGGG
GGTGTGGCCAGGGGCACCCGGGCATCGCCAGTCTAGCCACTCCTTCATAAAGCCCTCGCATCCAGGAGCGAGCAG
AGCCAGAGCAGGTTGGAGAGGAGACGCATCACCTCCGCTGCTCGCGGGGATCCTCTAGAAGCTTCGTTTAGTGAACC
GTCAGATCGCCTGGAGAGCCCATCCACGCTGTTTTGACCTCCATAGAAGACACCGGGACCGATCCAGCCTCCGCGGA
TTCGAATCCCGGGCGGAAACGGTGCATTGGAACCGCGGATTCCCCGTGCCAAGAGTGCAGTAAGTACCGCCTATAGAG
TCTATAGCCCCACAAAAAATGCTTTCTTTAATATACTTTTTTGTGTTTATCTTATTTCTAATACTTTCCCTAATC
TCTTTCTTTTCAGGGCAATAATGATACAATGTATCATGCCTCTTTGCACCATTCTAAAGAATAACAGTGATAAATTTCT
GGGTTAAGGCAATAGCAATATTTCTGCATATAAATATTTCTGCATATAAATTTGTAAGTGAATGTAAGAGGTTTCATAT
TGCTAATAGCAGCTACAATCCAGCTACCATTCTGCTTTTTATTTTTATGGTTGGGATAAGGCTGGATTATTCTGAGTCC
AAGCTAGGCCCTTTTGCTAATCATGTTTCATACCTCTTATCTTCTCCACAGCTCCTGGGCAACGTGCTGGTCTGTG
TGCTGGCCCATCACTTTGGCAAAGAATTGGGATTGCAACCGGTGCGCACCGGTCACCAAGCAGGAAGTCAAAGACTT
TTTCCGGTGGGCAAAGGATCACGTGGTTGAGGTGGAGCATGAATTCTACGTCAAAAAGGGTGGAGCCAAGAAAAGAC
CCGCCCCAGTGACGCAGATATAAGTGAGCCCAAACGGGTGCGCGAGTCAGTTGCGCAGCCATCGACGTCAGACGCG
GAAGCTTCGATCAACTACGCGGACAGGTACCAAAACAAATGTTCTCGTCACGTGGGCATGAATCTGATGCTGTTTCC
CTGCAGACAATGCGAGAGACTGAATCAGAATTCAAATATCTGCTTCACTCACGGTGTCAAAGACTGTTTAGAGTGCT
TTCCCGTGTGAGAATCTCAACCCGTTTCTGTGCTCAAAAAGGCGTATCAGAACTGTGCTACATTATCATCATGAT
GGAAAGGTGCCAGCCTTGCCTGCTTGGCAGCTGGTCAATGGGACTTGGATGACTGTGTTTCTGAACAATAAAT
GACTTAAACCAGGATAGGCTGCCGATGGTTATCTTCCAGATTGGCTCGAGGACAACCTTAGTGAAGGAATTCGCGAG
TGGTGGGCTTTGAAACCTGGAGCCCTCAACCCAAAGCAAAATCAACAACATCAAGACAACGCTCGAGGACTTTGTGCT
TCCGGGTTACAAATACCTTGGACCCGGCAACGGACTCGACAAGGGGGAGCCGGTCAACGCAGCAGACGCGGGGCC
TCGAGCACGACAAGGCTACGACCAGCAGCTCAAGGCCGGAGACAACCCGTACCTCAAGTACAACCACGCCGACGCC
GAGTTCCAGGAGCGGCTCAAAGAAGATACGTCTTTTGGGGCAACCTCGGGCGAGCAGTCTTCCAGGCCAAAAAGAG
GCTTCTTGAACCTCTTGGTCTGGTTGAGGAAGCGGCTAAGACGGCTCCTGGAAAGAAGAGGCTGTAGAGCAGTCTC
CTCAGGAACCGGACTCCTCCGCGGGTATTGGCAAATCGGGTGCACAGCCCGCTAAAAAGAGACTCAATTTCCGGTCA
ACTGGCGACACAGAGTCAGTCCAGACCCTCAACCAATCGGAGAACCTCCCGCAGCCCCCTCAGGTGTGGGATCTCT
TACAATGGCTTCCAGGTGGTGGCGCACCAGTGGCAGACAATAACGAAGGTGCCGATGGAGTGGGTAGTTCTCGGGAA
ATTGGCATTGCGATTCCCAATGGCTGGGGGACAGAGTCATCACCACCAGCACCCGAACCTGGGCCCTGCCACCTAC
AACAATCACCTCTACAAGCAAAATCTCCAACAGCACATCTGGAGGATCTTCAAATGACAACGCCTACTTCGGGTACAG
CACCCCTGGGGGATTTTTGACTTCAACAGATTCCACTGCCACTTCTCACCACGTGACTGGCAGCGACTCATCAACA
ACAACCTGGGGATTCGGCCCTAAGCGACTCAACTTCAAGCTCTTCAACATTCAGGTCAAAGAGGTTACGGCAACAAT
GGAGTCAAGACCATCGCCAATAACCTTACCAGCAGGTCAGGTCCTCAGGACTCAGACTATCAGCTCCCGTACGCT
GCTCGGGTCCGCTCACGAGGGCTGCCCTCCCGCGTCCCAGCGGACGTTTTTCATGATTCTCAGTACGGGTATCTGA
CGCTTAATGATGGAAGCCAGGCCGTGGGTGCTTTCGCTCTTTTACTGCTGGAATATTTCCCGTGCAGAAATGCTAAGA
ACGGGTAACAACCTTCCAGTTCAGCTACGAGTTTGGAGAAGCTACCTTTCCATAGCAGCTACGCTCACAGCCAAAGCCT
GGACCGACTAATGAATCCACTCATCGACCAATACTTGTACTATCTCTCAAAGACTATTAACGGTTCGGACAGAATC
AACAAACGCTAAAATTCAGTGTGGCCGGACCCAGCAACATGGCTGTCCAGGGAAGAACTACATACTGGACCCAGC
TACCGACAACAACGTGTCTCAACCACTGTGACTCAAAAACAACAACAGCGAATTTGCTTGGCCTGGAGCTTCTTCTTG

GGCTCTCAATGGACGTAATAGCTTGTATGAATCCTGGACCTGCTATGGCCAGCCACAAAGAAGGAGAGGACCGTTTCT
TTCCTTTGTCTGGATCTTTAATTTTTGGCAAACAAGGAACCTGGAAGAGACAACGTGGATGCGGACAAAGTCATGATA
ACCAACGAAGAAGAAATTAATACTAACCCTGAGCAACGGAGTCTATGGACAAGTGGCCACAAACCACAGAG
TGTACATCGATTGTTAATCAATAAACCGTTAATTCGTTTCAGTTGAACCTTTGGTCTCTGCGTATTTCTTTCTTATC
TAGTTTTCCATGGCTACGTAGATAAGTAGCATGGCGGGTTAATCATTAACTACAAGGAACCCTAGTGATGGAGTTGG
CCACTCCCTCTCTGCGCGCTCGCTCGCTCACTGAGGCCGGGCGACCAAGGTCGCCCGACGCCCGGGCTTTGCCCGG
GCGGCTCAGTGAGCGAGCGAGCGCGAGAGGGAGTGGCCAAGCATGCAATTAACTGGCCGTCGTTTTACAACGT
CGTGACTGGGAAAACCTGGCGTTACCCAACCTAATCGCCTTGCAGCACATCCCCCTTTGCCAGCTGTATCAGCAC
ACAATTGCCCATTTATACGCGCGTATAATGGACTATTGTGTGTGATAGCGTAATAGCGAAGAGGCCCGCACCGATCG
CCCTTCCCAACAGTTGCGCAGCCTGAATGGCGAATGGGACGCGCCCTGTAGCGGCGCATTAAAGCGCGGGCGGGTGTGG
TGTTTACGCGCAGCGTGACCGCTACACTTGCCAGCGCCCTAGCGCCCGCTCCTTTTCGCTTTCTTCCCTTCCCTTCTC
GCCACGTTCCGCCGGCTTTCCCGTCAAGCTCTAAATCGGGGGCTCCCTTTAGGGTTCGGATTTAGTGCTTTACGGCA
CCTCGACCCCAAAAACTTGATTAGGGTGATGGTTCACGTAGTGGGCCATCGCCCTGATAGACGGTTTTTTCGCCCTT
TGACGTTGGAGTCCACGTTCTTTAATAGTGGACTCTTGTTCAAAACCTGGAACAACACTCAACCCTATCTCGGTCTAT
TCTTTTGTATTTATAAGGGATTTTGGCGATTTCCGGCTATTGGTTAAAAAATGAGCTGATTTAACAAAAATTTAACGC
GAATTTTAAACAAAATATTAACGCTTACAATTTAGGTGGCACTTTTCGGGAAATGTGCGCGGAACCCCTATTGT
ATTTTTCTAAATACATTTCAAAATATGTATCCGCTCATGAGACAATAACCCTGATAAATGCTTCAATAATATTGAAAA
GGAAGAGTATGAGTATTCAACATTTCCGTGTCGCCCTTATTCCCTTTTTTTCGGCATTTCCTTCTGTTTTTGTCT
CACCCAGAAACGCTGGTGAAAGTAAAAGATGCTGAAGATCAGTTGGGTGCACGAGTGGGTTACATCGAACTGGATCT
CAACAGCGGTAAGATCCTTGAGAGTTTTTCGCCCGAAGAACGTTTTTCCAATGATGAGCACTTTTAAAGTTCTGCTAT
GTGGCGCGGTATTATCCCGTATTGACGCCGGGCAAGAGCAACTCGGTGCGCGCATACTATTCTCAGAATGACTTG
GTTGAGTACTCACAGTACAGAAAAGCATCTTACGGATGGCATGACAGTAAGAGAATTATGCAGTGTGCCATAAC
CATGAGTGATAACACTGCGGCCAACTTACTTCTGACAACGATCGGAGGACCGAAGGAGCTAACCGCTTTTTTGCACA
ACATGGGGGATCATGTAACCTCGCCTTGATCGTTGGGAACCGGAGCTGAATGAAGCCATAACAAACGACGAGCGTGAC
ACCACGATGCCTGTAGCAATGGCAACAACGTTGCGCAAACTATTAACTGGCGAACTACTTACTCTAGCTTCCCGGCA
ACAATTAATAGACTGGATGGAGGCGGATAAAGTTGCAGGACCCTTCTGCGCTCGGCCCTTCCGGCTGGCTGGTTTTA
TTGCTGATAAATCTGGAGCCGGTGAGCGTGGGTCTCGCGGTATCATTGCAGCACTGGGGCCAGATGGTAAGCCCTCC
CGTATCGTAGTTATCTACAGGACGGGGAGTCAGGCAACTATGGATGAACGAAATAGACAGATCGCTGAGATAGGTGC
CTCACTGATTAAGCATTGGTAACTGTGACACCAAGTTACTCATATATACTTTAGATTGATTTAAAACCTTCATTTTT
AATTTAAAAGGATCTAGGTGAAGATCCTTTTTGATAATCTCATGACCAAAATCCCTAACGTGAGTTTTTCGTTCCAC
TGAGCGTCAGACCCCGTAGAAAAGATCAAAGGATCTTCTTGAGATCCTTTTTTTCTGCGCGTAATCTGCTGCTTGCA
AACAAAAAACACCAGCTACCAGCGGTGGTTTTGTTTGCAGGATCAAGAGCTACCAACTCTTTTTCCGAAGGTAACCTG
GCTTCAGCAGAGCGCAGATACCAAATACTGTTCTTCTAGTGTAGCCGTAGTTAGGCCACCACTTCAAGAACTCTGTA
GCACCGCTACATACCTCGCTCTGCTAATCCTGTTACCAGTGGCTGCTGCCAGTGGCGATAAGTCGTGTCTTACCGG
GTTGGACTCAAGACGATAGTTACCGGATAAGGCGCAGCGGTGCGGCTGAACGGGGGGTTCGTGCACACAGCCAGCT
TGGAGCGAACGACCTACACCGAACTGAGATACCTACAGCGTGAGCTATGAGAAAGCGCCACGCTTCCCGAAGGGAGA
AAGGCGGACAGGTATCCGGTAAGCGGCAGGGTCGGAACAGGAGAGCGCACGAGGGAGCTTCCAGGGGGAAACGCCTG
GTATCTTTATAGTCTGTGCGGTTTTGCCACCTCTGACTTGAGCGTCGATTTTTTGTGATGCTCGTCAGGGGGGCGGA
GCCTATGGAAAAACGCCAGCAACGCGGCCTTTTTACGGTTCCTGGCCTTTTGTGCTGGCCTTTTGTCTCACATGTTCTTT
CCTGCGTTATCCCCTGATTCTGTGGATAACCGTATTACCGCCTTTGAGTGAGCTGATACCGCTCGCCGAGCCGAAC
GACCGAGCGCAGCGAGTCAGTGAGCGAGGAAGCGGAAGAGCGCCCAATACGCAAACCGCCTTCCCCGCGCGTTGGC
CGATTCATTAATGTCTAGATATCAGCACACAATAGTCCATTATACGCGCGTATAATGGGCAATTGTGTGTGATACA
GCTGGCACGACAGGTTTTCCGACTGGAAAGCGGGCAGTGAGCGCAACGCAATTAATGTGAGTTAGCTCACTCATTAG
GCACCCAGGCTTTACACTTTATGCTTCCGGCTCGTATGTTGTGTGGAATTGTGAGCGGATAACAATTTACACACAGG
AAACAGCTATGACCATGATTACGCCAGATTTAATTAAGG

pREP-3stop

Features:

- 68-1933: AAV2 REP ORF
- 1950-3703: AAV9 CAPA Fragment
- 1965-1967: Premature VP1 stop codon
- 2376-2378: Premature VP2 stop codon
- 2595-2597: Premature VP3 stop codon
- 3520-3525: MscI restriction site
- 5207-6067: Ampicillin Resistance

GTCGACGGTATCGGGGGAGCTCGCAGGGTCTCCATTTTGAAGCGGGAGGTTTGAACGCGCAGCCGCCATGCCGGGGT
TTTACGAGATTGTGATTAAGGTCCCAGCGACCTTGACGAGCATCTGCCCGGCATTTCTGACAGCTTTGTGAACTGG
GTGGCCGAGAAGGAATGGGAGTTGCCGCCAGATTCTGACATGGATCTGAATCTGATTGAGCAGGCACCCCTGACCGT
GGCCGAGAAGCTGCAGCGCGACTTTCTGACGGAATGGCGCCGTGTGAGTAAGGCCCGGAGGCTCTTTTCTTTGTGC
AATTTGAGAAGGGGAGAGAGCTACTTCCACATGCACGTGCTCGTGGAAACCACCGGGGTGAAATCCATGGTTTTGGGA
CGTTTCTCTGAGTCAGATTCCGCGAAAAACTGATTTCAGAGAATTTACCGCGGGATCGAGCCGACTTTGCCAAACTGGTT
CGCGGTACAAAAGACCAGAAATGGCGCCGGAGCGGAACAAGGTGGTGGATGAGTGCTACATCCCAAACTTACTTGC
TCCCCAAAACCCAGCCTGAGCTCCAGTGGGCGTGGACTAATATGGAACAGTATTTAAGCGCCTGTTTGAATCTCACG
GAGCGTAAACGGTTGGTGGCGCAGCATCTGACGCACGTGTGCGAGACGCAGGAGCAGAACAAGAGAATCAGAATCC
CAATTCTGATGCGCCGGTGTATCAGATCAAAAACTTCAGCCAGGTACATGGAGCTGGTTCGGGTGGCTCGTGGACAAGG
GGATTACCTCGGAGAAGCAGTGGATCCAGGAGGACCAGGCCTCATACATCTCCTTCAATGCGGCCTCCAACCTCGCGG
TCCCCAAATCAAGGCTGCCTTGGACAATGCGGGAAAGATTATGAGCCTGACTAAAACCGCCCCGACTACCTGGTGGG
CCAGCAGCCCCTGGAGGACATTTCCAGCAATCGGATTTATAAAATTTTGGAACTAAACGGGTACGATCCCCAATATG
CGGCTTCCGTCTTTCTGGGATGGGCCACGAAAAAGTTTCGGCAAGAGGAACACCATCTGGCTGTTTGGGCCTGCAACT
ACCGGGAAGACCAACATCGCGGAGGCCATAGCCACACTGTGCCCTTCTACGGGTGCGTAAACTGGACCAATGAGAA
CTTTCCCTTCAACGACTGTGTGCAAGATGGTGTATCTGGTGGGAGGAGGGGAAGATGACCGCCAAGGTCTGTGGAGT
CGGCCAAAGCCATTCTCGGAGGAAGCAAGGTGCGCGTGGACCAGAAATGCAAGTCTCGGCCCAGATAGACCCGACT
CCCCGTGATCGTCACTCCAACCAACATGTGCGCCGTGATTGACGGGAACCAACGACCTTCGAACACCCAGCAGCC
GTTTGCAAGACCGGATGTTCAAATTTGAACCTACCCCGCTGCTGGATCATGACTTTGGGAAGTCAACCAAGCAGGAAG
TCAAAGACTTTTTCCGGTGGGCAAAGGATCACGTGGTTGAGGTGGAGCATGAATTTCTACGTCAAAGGGTGGAGCC
AAGAAAAGACCCGCCCCAGTGACGCAGATATAAGTGAGCCCAAACGGGTGCGCGAGTCAGTTGCGCAGCCATCGAC
GTCAGACGCGGAAGCTTCGATCAACTACGCGGACAGGTACCAAAAACAAATGTTTCTCGTCACGTGGGCATGAATCTGA
TGCTGTTTTCCCTGCAGACAATGCGAGAGACTGAATCAGAATTCAAATATCTGCTTCACTCACGGTGTCAAAGACTGT
TTAGAGTGCTTTCCCGTGTGAGAATCTCAACCCGTTTTCTGTGCTCAAAAAGGCGTATCAGAAACTGTGCTACATTCA
TCACATCATGGGAAAGGTGCCAGACGCTTGCACCTGCTTGCACCTGGTCAATGTGGACTTGGATGACTGTGTTTTCTG
AACAATAAATGACTTAAACCAGGTATGGCTGCCGATGGTTAGCTTCCAGATTGGCTCGAGGACAACCTTAGTGAAGG
AATTCGCGAGTGGTGGGCTTTGAAACCTGGAGCCCTCAACCCAAGGCAAATCAACAACATCAAGACAACGCTCGAG
GTCTTGTGCTTCCGGGTTACAAATACCTTGGACCCGGCAACGGACTCGACAAGGGGGAGCCGGTCAACGCAGCAGAC
GCGGCGGCCCTCGAGCACGACAAGGCCTACGACCAGCAGCTCAAGGCCGGAGACAACCCGTACCTCAAGTACAACCA
CGCCGACGCGGAGTTCAGGAGCGGCTCAAAGAAGATACGTCTTTTGGGGCAACCTCGGGCGAGCAGTCTTCCAGG
CCAAAAGAGGCTTCTTGAACCTCTTGGTCTGGTTGAGGAAGCGGCTAAGACGGCTCCTGGAAAGTAGAGGCCTGTA
GAGCAGTCTCCTCAGGAACCGGACTCCTCCGCGGATTTGGCAAATCGGGTGCACAGCCCGCTAAAAAGAGACTCAA
TTTCGGTTCAGACTGGCGACACAGAGTCAGTCCAGACCCTCAACCAATCGGAGAACCCTCCCGCAGCCCCCTCAGGTG
TGGGATCTCTTACAATGGCTTTCAGGTGGTGGCGCACCAGTGGCAGACAATAACTTAAAGGTGCCGATGGAGTGGGTAGT
TCCTCGGGAATTTGGCATTGCGATTCCCAATGGCTGGGGGACAGAGTCATCACCACCAGCACCCGAACCTGGGCCCT
GCCACCTACAACAATCACCTCTACAAGCAAATCTCCAACAGCACATCTGGAGGATCTTCAAATGACAACGCCTACT
TCGGCTACAGCACCCCTGGGGTATTTTACTTCAACAGATTCCACTGCCACTTCTCACCACGTGACTGGCAGCGA
CTCATCAACAACAACCTGGGGATTCCGGCCTAAGCGACTCAACTTCAAGCTCTTCAACATTCAGGTCAAAGAGGTTAC
GGACAACAATGGAGTCAAGACCATCGCCAATAACCTTACCAGCACGGTCCAGGTCTTACGGACTCAGACTATCAGC
TCCCCTACGTGCTCGGGTCCGGTCCAGAGGGTGCCTCCCGCCGTTCCAGCGGACGTTTTTCATGATTCTCAGTAC
GGGTATCTGACGCTTAATGATGGAAGCCAGGCCGTGGGTGCTTTCGTCTTTTACTGCCTGGAATATTTCCCGTGC
AATGCTAAGAACGGGTAACAACCTTCCAGTTCAGCTACGAGTTTGGAGAACGTACCTTTCCATAGCAGCTACGCTCACA
GCCAAAGCCTGGACCCGACTAATGAATCCACTGTATCGACCAATACTTGTACTATCTCTCAAAGACTATTAACGGTTCT
GGACAGAATCAACAACAGCTAAAATTCAGTGTGCGCCGGACCCAGCAACATGGCTGTCCAGGAAGAAACTACATACC
TGGACCCAGTACCACACAACAGTGTCTCAACCCTGTGACTCAAAAACAACAACAGCAGCAATTTGCTTGGCCTGGAG
CTTCTTCTTGGGCTCTCAATGGACGTAATAGCTTGTGTAATCCTGGACCTGCTAAGGCCAAGTCAGCGTGGAGATCG
AGTGGGAGCTGCAGAAGGAAAACAGCAAGCGCTGGAACCCGGAGATCCAGTACACTTCCAACCTATTACAAGTCTAAT
AATGTTGAATTTGCTGTTAATACTGAAGGTGTATATAGTGAACCCCGCCCCATTGGCACAGATACCTGACTCGTAA
TCTGTAAATTGCTTGTTAATCAATAAACCGTTTTAATTCGTTTTAGTTGAACCTTTGGTCTCTGCGAAGGGCGAATTCGT

TTAAACCTGCAGGACTAGAGTCCTGTATTAGAGGTCACGTGAGTGTTTTGCGACATTTTGGACACCATGTGGTCAC
GCTGGGTATTTAAGCCCGAGTGAGCACGCAGGGTCTCCATTTTGAAGCGGGAGGTTTGAACGCGCAGCCGCAAGCC
GAATTTGCAGATATCCATCACACTGGCGGGCGCTCGACTAGAGCGGGCCACCGCGGTGGAGCTCCAGCTTTTGT
TCCCTTTAGTGAGGGTTAATTGCGCGCTTGGCGTAATCATGGTCATAGCTGTTTCTGTGTGAAATTTGTTATCCGCT
CACAATTCACACAACATAACGAGCCGGAAGCATAAAGTGTAAGCCTGGGGTGCCTAATGAGTGAGCTAACTCACAT
TAATTGCGTTGCGCTCACTGCCCGCTTTCCAGTCGGGAAACCTGTCGTGCCAGCTGCATTAATGAATCGGCCAACGC
GCGGGGAGAGGGGTTTTGCGTATTGGGCGCTCTTCCGCTTCTCGCTCACTGACTCGCTGCGCTCGGTGCTTCCGCT
GCGGCGAGCGGTATCAGCTCACTCAAAGGCGGTAATACGGTTATCCACAGAATCAGGGGATAACGCAGGAAAGAACA
TGTGAGCAAAAGGCCAGCAAAAGGCCAGGAACCGTAAAAAGGCCGCGTTGCTGGCGTTTTTCCATAGGCTCCGCCCC
CCTGACGAGCATCAAAAAATCGACGCTCAAGTCAGAGGTGGCGAAACCCGACAGGACTATAAAGATAACCAGGCGTT
TCCCCCTGGAAGCTCCCTCGTGCGCTCTCTGTTCCGACCCTGCCGCTTACCGGATACCTGTCCGCCTTTCTCCCTT
CGGAAGCGTGGCGCTTTCTCATAGCTCACGCTGTAGGTATCTCAGTTCGGTGTAGGTCGTTCCGCTCCAAGCTGGGC
TGTGTGCACGAACCCCCGTTTCCAGCCCGACCGCTGCGCCTTATCCGGTAACTATCGTCTTGAGTCCAACCCGGTAAG
ACACGACTTATCGCCACTGGCAGCAGCCACTGGTAACAGGATTAGCAGAGCGAGGTATGTAGGCGGTGCTACAGAGT
TCTTGAAGTGGTGGCCTAACTACGGCTACACTAGAAGAACAGTATTTGGTATCTGCGCTCTGCTGAAGCCAGTTACC
TTCGGA AAAAGAGTTGGTAGCTCTTGATCCGGCAAACAAACCACCGCTGGTAGCGGTGGTTTTTTTTGTTTGAAGCA
GCAGATTACGCGCAGAAAAAAGGATCTCAAGAAGATCCTTTGATCTTTTCTACGGGGTCTGACGCTCAGTGGAACG
AAAACCTCACGTTAAGGGATTTTTGGTCATGAGATTATCAAAAAGGATCTTACCTAGATCCTTTTAAATTA AAAATGA
AGTTTTAAATCAATCTAAAGTATATATGAGTAAACTTGGTCTGACAGTTACCAATGCTTAAATCAGTGAGGCACCTAT
CTCAGCGATCTGTCTATTTTCGTTTCCATCCATAGTTGCCTGACTCCCCGTCGTGTAGATAACTACGATACGGGAGGGCT
TACCATCTGGCCCCAGTGCTGCAATGATAACCGCGAGACCCACGCTCACCGGCTCCAGATTTATCAGCAATAAACCCAG
CCAGCCGGAAGGGCCGAGCGCAGAAGTGGTCTTGCAACTTTATCCGCTCCATCCAGTCTATTAATTGTTGCGGGGA
AGCTAGAGTAAGTAGTTCCGCCAGTTAATAGTTTTGCGCAACGTTGTTGCCATTGCTACAGGCATCGTGGTGTACGCT
CGTCGTTTTGGTATGGCTTCATTCAGCTCCGTTCCCAACGATCAAGGCGAGTTACATGATCCCCCATGTTGTGCAAA
AAAGCGGTTAGCTCCTTCGGTCTCCGATCGTTGTGAGAAGTAAGTTGGCCGAGTGTATCACTCATGGTTATGGC
AGCACTGCATAATTTCTTACTGTGTCATGCCATCCGTAAGATGCTTTTTCTGTGACTGGTGAGTACTCAACCAAGTCAT
TCTGAGAATAGTGTATGCGGGCAGCCGAGTTGCTCTTGCCCGGGCGTCAATACGGGATAATACCGCGCCACATAGCAGA
ACTTTAAAAGTGTCTCATCTTGGAAAACGTTCTTCCGGGGCGAAAACCTCAAGGATCTTACCAGCTGTTGAGATCCAG
TTCGATGTAACCCACTCGTGCACCCAACCTGATCTTTCAGCATCTTTTACTTTTACCAGCGTTTCTGGGTGAGCAAAA
CAGGAAGGC AAAATGCCGCAAAAAAGGGAATAAGGGCGACACGGAAATGTTGAATACTCATACTCTTCCCTTTTCAA
TATTATTGAAGCATTATCAGGGTTATTGTCTCATGAGCGGATACATATTTGAATGTATTTAGAAAAATAAACAAAT
AGGGGTTCCGCGCACATTTCCCCGAAAAGTGCCACCTAAATTTGTAAGCGTTAATATTTTGTAAAATTCGCGTTAAA
TTTTTGTAAAATCAGCTCATTTTTTTAACCAATAGGCCGAAATCGGCAAAATCCCTTATAAATCAAAAAGAAATAGACCG
AGATAGGGTTGAGTGTGTTCCAGTTTGGAAACAAGAGTCCACTATTAAGAACGTGGACTCCAACGTCAAAGGGCGA
AAAACCGTCTATCAGGGCGATGGCCCACTACGTGAACCATCACCTAATCAAGTTTTTTGGGGTTCGAGGTGCCGTAA
AGCACTAAATCGGAACCTAAAGGGAGCCCCGATTTAGAGCTTGACGGGGAAAGCCGGCGAACGTGGCGAGAAAGG
AAGGGAAGAAAGCGAAAGGAGCGGGCGCTAGGGCGCTGGCAAGTGTAGCGGTCACGCTGCGCGTAACCACCACACCC
GCCGCGCTTAAATGCGCCGCTACAGGGCGCGTCCCATTCCGCATTTCAGGCTGCGCAACTGTTGGGAAGGGCGATCGGT
GCGGGCCTCTTCGCTATTACGCCAGCTGGCGAAAGGGGGATGTGCTGCAAGGCGATTAAGTTGGGTAACGCCAGGGT
TTTCCCAGTCACGACGTTGTA AAAACGACGGCCAGTGAGCGCGGTAATACGACTCACTATAGGGCGAATTGGGTACC
GGCCCCCCCCCTCGATCGAG

scAAV-CAG-EGFP

Features:

- 1-105: Left trsΔITR
- 138-796f: CMV/CBA Promoter
- 817-1382: Hybrid CMV-Globin intron
- 1404-2135: EGFP
- 2143-2211: TK2 polyadenylation sequence
- 2248-2377: Right ITR
- 3140-4000: Ampicillin Resistance

CTGCGCGCTCGCTCGCTCACTGAGGCCGCCCGGGCAAAGCCCGGGCGTCCGGGCGACCTTTGGTCCGCCGGCCTCAGT
GAGCGAGCGAGCGCGCAGAGAGGGAGTGTAGCCATGCTCTAGGAAGATCAATTCAATTCACGCGTTCGACATTGATTA
TTGACTAGTTATTAATAGTAATCAATTACGGGGTCATTAGTTTCATAGCCCATATATGGAGTTCGCGGTTACATAACT
TACGGTAAATGGCCCGCTGGCTGACCGCCCAACGACCCCCGCCATTGACGTCAATAATGACGTATGTTCCCATAG
TAACGCCAATAGGGACTTTCCATTGACGTCAATGGGTGGAGTATTTACGGTAAACTGCCCACTTGGCAGTACATCAA
GTGTATCATATGCCAAGTACGCCCCCTATTGACGTCAATGACGGTAAATGGCCCGCTGGCATTATGCCCAGTACAT
GACCTTATGGGACTTTCCCTACTTGGCAGTACATCTACGTATTAGTCAATCGTATTACCATGTTCGAGGCCACGTTCTG
CTTCACTCTCCCCATCTCCCCCCCCCTCCCCACCCCAATTTTGTATTTATTTATTTTTTAATTTTTTGTGCAGCGA
TGGGGGCGGGGGGGGGGGCGCGCGCCAGGCGGGGCGGGGCGGGGCGAGGGGCGGGGCGGGGCGAGGCGGAGAGGTG
CGGCGGCAGCCAATCAGAGCGGCGCGCTCCGAAAGTTTCTTTTTATGGCGAGGCGGCGGGCGGGCCCTATAAAA
AAGCGAAGCGCGCGGGCGGGGAGCAAGCTTCGTTTGTAGTGAACCGTCAGATCGCCTGGAGACGCCATCCACGCTGT
TTTGACCTCCATAGAAGACACCGGGACCGATCCAGCCTCCGCGGATTTCGAATCCCGGCCGGGAACGGTGCATTGGAA
CGCGGATTCCCCGTGCCAAGAGTGACGTAAGTACCGCCTATAGAGTCTATAGGCCACAAAAAATGCTTTCTTCTTT
TAATATACTTTTTTGTATCTTATTTCTAATACTTTCCCTAATCTCTTTCTTTTCAGGGCAATAATGATACAATGTA
TCATGCCTCTTTGCACCATTCTAAAGAATAACAGTGATAATTTCTGGGTAAAGGCAATAGCAATATTTCTGCATATA
AATATTTCTGCATATAAATTTGTAAGTGTAAAGAGTTTCATATTGCTAATAGCAGCTACAATCCAGCTACCATTCT
TGCTTTTATTTTTATGGTTGGGATAAGGCTGGATTATTCTGAGTCCAAGCTAGGCCCTTTTGTAAATCATGTTCCATAC
CTCTTATCTCTCCACAGCTCCTGGGCAACGCTGGTCTGTGTGTGGGCCATCACTTTGGCAAGAATTTGGGA
TTTCAACCGGTTGCCACCATTGGTGAGCAAGGCGAGGAGCTGTTTACCGGGTGGTGGCCCTCTGTTGCGAGCTGGAC
GGCAGCTAAACGGCCACAAGTTTCAAGCTGCGGCGAGGGCGAGGGCGATGCCACCTACGGCAAGCTGACCCTGAA
GTTTCACTGCACCACCGCAAGCTGCCCGTGGCCACCTCGTGACCACCTGACCTACGGCGTGCAGTGTCT
TCAGCCGCTACCCCGACCACATGAAGCAGCAGCACTTCTTCAAGTCCGCCATGCCCGAAGGCTACGTCCAGGAGCGC
ACCATCTTCTTCAAGGACGACGGCAACTACAAGACCCGCGCCGAGGTGAAGTTTCGAGGGCGACACCCTGGTGAACCG
CATCGAGCTGAAGGGCATCGACTTCAAGGAGGACGGCAACATCTGGGGCACAAGCTGGAGTACAACACTACAACAGCC
ACAACGTCTATATCATGGCCGACAAGCAGAAGAACGGCATCAAGGTGAACCTTCAAGATCCGCCACAACATCGAGGAC
GGCAGCGTGCAGCTCGCCGACCACTACCAGCAGAACACCCCATCGGGCAGCGCCCCGTGCTGCTGCCGACAACCA
CTACCTGAGCACCCAGTCCGCCCTGAGCAAAGACCCCAACGAGAAGCGCGATCACATGGTCTGCTGGAGTTCGTGA
CCGCCCGCGGGATCACTCTCGGCATGGACGAGCTGTACAAGTCCGGACTCAGATAGTCTCGAGTGGCCGCAATAAAA
TATCTTTATTTTTATTACATCTGTGTGTTGGTTTTTTGTGTGAGGATCTCCTAGGTAGATAAGTAGCATGGCGGGTT
AATCATTAACTACAAGGAACCCCTAGTGTGGAGTTGGCCACTCCCTCTCTGCGCGCTCGCTCGCTCACTGAGGCCG
GGCGACCAAGGTCGCCCGACGCCCGGGCTTTGCCCGGGCGGCTCAGTGAGCGAGCGAGCGCGAGCCTTAATTA
CCTAATTCAGTGGCCGTGTTTTACAACGTGCTGACTGGGAAAACCCCTGGCGTTACCCCACTTAATCGCCTTGACG
ACATCCCCTTTTCGCGAGCTGGCGTAATAGCGAAGAGGCCCGACCCGATCGCCCTTCCCAACAGTTGCGCAGCCTGA
ATGGCGAATGGGACGCGCCCTGTAGCGGCGCATTAAAGCGCGGGCGGGTGTGGTGGTTACGCGCAGCGTGACCGCTACA
CTTGCCAGCGCCCTAGCGCCGCTCCTTTTCGCTTTCTTCCCTTCTTTCTCGCCACGTTTCGCCGGCTTTCCCCGTCA
AGCTCTAAATCGGGGGCTCCCTTTAGGGTTCGGATTTAGTGTCTTACGGCACCTCGACCCCAAAAACTTGATTAGG
GTGATGGTTCACGTAGTGGGCCATCGCCCTGATAGACGGTTTTTTCGCCCTTTGACGTTGGAGTCCACGTTCTTTAAT
AGTGGACTCTTGTTCCAAACCTGGAACAACACTCAACCCTATCTCGGTCTATTCTTTTGTATTTATAAGGGATTTTGCC
GATTTCCGCCCTATTGGTTAAAAAATGAGCTGATTTAAACAAAAATTTAACGCGAATTTTAAACAAAAATTTAACGCTTA
CAATTTAGGTGGCACTTTTCGGGAAATGTGCGCGGAACCCCTATTTGTTTATTTTTCTAAATACATTCAAATATGT
ATCCGCTCATGAGACAATAACCCCTGATAAATGCTTCAATAATATTGAAAAAGGAAGAGTATGAGTATTCAACATTTT
CGTGTGCCCTTATTCCCTTTTTTTCGGGCATTTTTGCCTTCCCTGTTTTTGTCTACCCAGAAAACGCTGGTGAAGTAAA
AGATGCTGAAGATCAGTTGGGTGCACGAGTGGGTACATCGAAGTGGATCTCAACAGCGGTAAGATCTTTGAGAGTT
TTCGCCCCGAAGAAGCTTTTCCAATGATGAGCACTTTTAAAGTTCTGCTATGTGGCGCGGCTATTATCCCGTATGAC
GCCGGGCAAGAGCAACTCGGTCCCGCATACACTATTTTAAAGTTCTGCTATGTGGCGCGGCTATTATCCCGTATGAC
GCATCTTACGGATGGCATGACAGTAAGAGAATTATGCAAGTGTGCCATAACCATGAGTGATAACACTGCGGCCAACT
TACTTCTGACAACGATCGGAGGACCGAAGGAGCTAACCGCTTTTTTTCACAACATGGGGGATCATGTAACCTCGCCTT
GATCGTTGGGAACCGGAGCTGAATGAAGCCATACCAAACGACGAGCGTGACACCACGATGCCTGTAGCAATGGCAAC
AACGTTGCGCAAACCTATTAACCTGGCGAACTACTTACTCTAGCTTCCCGGCAACAATTAATAGACTGGATGGAGGCGG

ATAAAGTTGCAGGACCACTTCTGCGCTCGGCCCTTCCGGCTGGCTGGTTTTATTGCTGATAAAATCTGGAGCCGGTGAG
CGTGGGTCTCGCGGTATCATTGCAGCACTGGGGCCAGATGGTAAGCCCTCCCGTATCGTAGTTATCTACACGACGGG
GAGTCAGGCAACTATGGATGAACGAAATAGACAGATCGCTGAGATAGGTGCCTCACTGATTAAGCATTGGTAACTGT
CAGACCAAGTTTACTCATATATACTTTAGATTGATTTAAAACCTCATTTTTAATTTAAAAGGATCTAGGTGAAGATC
CTTTTTGATAATCTCATGACCAAAATCCCTTAACGTGAGTTTTCGTTCCACTGAGCGTCAGACCCCGTAGAAAAGAT
CAAAGGATCTTCTTGAGATCCTTTTTTTCTGCGCGTAATCTGCTGCTTGCAAACAAAAAACCACCGCTACCAGCGG
TGGTTTGTGGCCGGATCAAGAGCTACCAACTCTTTTTCCGAAGGTAAGTGGCTTCAGCAGAGCGCAGATACCAAT
ACTGTTCTTCTAGTGTAGCCGTAGTTAGGCCACCACTTCAAGAACTCTGTAGCACCGCCTACATACCTCGCTCTGCT
AATCCTGTTACCAGTGGCTGCTGCCAGTGGCGATAAGTCGTGTCTTACCGGGTTGGACTCAAGACGATAGTTACCGG
ATAAGGCGCAGCGGTCTGGGCTGAACGGGGGGTTCGTGCACACAGCCAGCTTGGAGCGAACGACCTACACCGAACTG
AGATACCTACAGCGTGAGCTATGAGAAAGCGCCACGCTTCCCGAAGGGAGAAAGGCGGACAGGTATCCGGTAAGCGG
CAGGGTCGGAACAGGAGAGCGCACGAGGGGAGCTTCCAGGGGAAACGCCTGGTATCTTTATAGTCCTGTCTGGGTTTC
GCCACCTCTGACTTGAGCGTCGATTTTTGTGATGCTCGTCAGGGGGCGGAGCCTATGGAAAAACGCCAGCAACGCG
GCCTTTTTACGGTTCCTGGCCTTTTGCTGGCCTTTTGCTCACATGTTCTTTTCTGCGTTATCCCCTGATTCTGTGGA
TAACCGTATTACCGCCTTTGAGTGAGCTGATACCGCTCGCCGAGCCGAACGACCGAGCGCAGCGAGTCAGTGAGCG
AGGAAGCGGAAGAGCGCCCAATACGCAAACCGCCTCTCCCCGCGCGTTGGCCGATTCAATTAATGCAGCTGGCAGC
AGGTTTCCCGACTGGAAAGCGGGCAGTGAGCGCAACGCAATTAATGTGAGTTAGCTCACTCATTAGGCACCCAGGC
TTTACACTTTATGCTTCCGGCTCGTATGTTGTGTGGAATTGTGAGCGGATAACAATTTACACAGGAAACAGCTATG
ACCATGATTACGCCAGATTTAATTAAGGCCTTAATTAGG